Experimental evaluation of two complementary decentralized event-based control methods

Manuela Sigurani, C. Stöcker, Lars Grüne, J. Lunze

Experimental evaluation of two complementary decentralized event-based control methods

M. Sigurani[a], C. Stöcker[b,*], L. Grüne[a], J. Lunze[b]

[a] *University of Bayreuth, Mathematical Institute, Germany*
[b] *Ruhr-University Bochum, Institute of Automation and Computer Control, Germany*

Abstract

Event-based control aims at the reduction of the feedback communication effort among the sensors, controllers and actuators in control loops. The feedback communication is invoked by some well-defined triggering condition. This paper presents a new method for the decentralized event-based control of physically interconnected systems and shows its experimental evaluation. The novel method is based on two complementary approaches, called the global and the local approach, which jointly ensure the ultimate boundedness of the closed-loop system. The global approach steers the state of each subsystem into a target region, whereas the local approach makes the state remain in this set in spite of exogenous disturbances and the effect of the interconnections to other subsystems. This event-based control method is applied to a continuous flow process to show its practical implementation and to evaluate the analytical results on the basis of experiments.

Keywords: Event-based control, Ultimate boundedness, Networked control

*Corresponding author
Email addresses: manuela.sigurani@uni-bayreuth.de (M. Sigurani), stoecker@atp.rub.de (C. Stöcker), lars.gruene@uni-bayreuth.de (L. Grüne), lunze@atp.rub.de (J. Lunze)

1. Introduction

In event-based control the communication among the components of a control system is restricted to time instants at which the exchange of current information is necessary to ensure a desired behavior of the closed-loop system. Its triggering scheme contrasts with the current practice, where the controller is implemented on digital hardware and the control task is executed periodically (sampled-data control). As the main reason for using this kind of implementation, the analysis and design of sampled-data control loops can be based on a well-established theory. However, the periodic sampling, computing and updating of actuator signals is carried out whether required or not, which can lead to a waste of communication resources. To use these communication resources more efficiently, event-based control has been proposed as an alternative to periodic control.

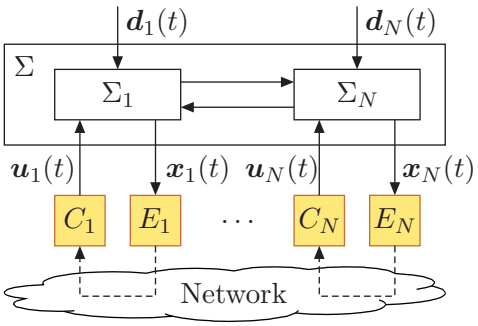

Figure 1: Structure of the event-based control system

This paper investigates decentralized event-based control of interconnected systems Σ_i $(i = 1, \ldots, N)$ (Fig. 1). The event-based controller for

each subsystem Σ_i consists of an event generator E_i and a control input generator C_i which communicate over a network only at certain event times. The aim of this paper is twofold: First, it is presented how two approaches to decentralized event-based control can be combined to jointly accomplish ultimate boundedness of the overall control system. These two approaches, which are subsequently specified as the *global approach* and the *local approach* to decentralized event-based control, are based on methods which have been recently published by Grüne & Sigurani (2013) and Stöcker et al. (2013), respectively. The global approach drives the state of each subsystem into a target region in finite time where the local approach takes over and keeps the state within this region in spite of exogenous disturbances or interconnections to other systems. The second aim of this paper is to demonstrate how these complementary approaches are applied in practice to a continuous flow process. The analytical results derived in the first part of this paper are evaluated by experiments.

Event-based control is a useful means to reduce the communication while accomplishing a desired control performance which has been shown in several simulation and experimental studies, e.g. by Hendricks et al. (1994); Heemels et al. (1999); Kwon et al. (1999); Yook et al. (2002); Sandee et al. (2007); Henningsson & Cervin (2009); Lehmann & Lunze (2011); Trimpe & D'Andrea (2011). Besides the investigation of the practical applicability, a lot of effort has been spend on developing a profound theory on event-based control starting with the works of Arzén (1999); Åström & Bernhardsson (1999) and has been continued in recent years, e.g. by Tabuada (2007); Henningsson et al. (2008); Gawthrop & Wang (2009); Lunze & Lehmann

(2010); Yu & Antsaklis (2011); Donkers & Heemels (2012); Wang & Lemmon (2012); Molin & Hirche (2013). Most of the literature on event-based control is concerned with stabilization. The problem of rendering the system asymptotically or exponentially stable using event-based feedback has been studied, among others, by Tabuada (2007); Mazo & Tabuada (2010); De Persis et al. (2011); Garcia & Antsaklis (2011); Wang & Lemmon (2012). Except for the works of Wang & Lemmon (2011a) and Stöcker & Lunze (2013), the price for asymptotic stability is usually a more frequent communication the cl! oser the state converges to the desired target point. Moreover, the event-based control approaches which achieve asymptotic stability do not tolerate model uncertainties or exogenous disturbances.

¿From a practical perspective it is more preferable to steer the system state into a target region, rather than a point, and maintain it there, which is known in literature as *ultimate boundedness* (see e.g. Khalil (2002)). Event-based control approaches which aim at this property have been presented by Lunze & Lehmann (2010); Grüne et al. (2010); Lehmann (2011); Tallapragada & Chopra (2011); Wang & Lemmon (2011b); Donkers & Heemels (2012) where the last two references proposed approaches that render the control system $\mathcal{L}_p$-stable or $\mathcal{L}_\infty$-stable, respectively. According to the definition of ultimate boundedness (Khalil (2002)) the state must enter the target set within some finite time T and remain there for all $t \geq T$. However, in none of the publications that study ultimate boundedness of event-based control systems (Grüne et al. (2010); Lehmann (2011); Tallapragada & Chopra (2011)), the time T (or a bound on it) is derived. In contrast, this paper gives an upper bound on the time T in which the state reaches the target

set.

While early works on event-based control mainly have been focused on single-loop systems, some recent publications deal with decentralized control (Mazo & Tabuada (2010); Stöcker et al. (2013); Garcia & Antsaklis (2012)) or distributed control (Wang & Lemmon (2011b); De Persis et al. (2011)). In the existing literature the plant is considered to be exclusively described by either nonlinear dynamics (Tabuada (2007); Mazo & Tabuada (2010); De Persis et al. (2011); Stöcker & Lunze (2011); Wang & Lemmon (2012) Grüne & Müller (2009)) or by linear dynamics (Lunze & Lehmann (2010); Donkers & Heemels (2012)). The approach presented in this paper uses both a nonlinear model for the global approach and a linearized model for the local approach. In this way, this paper follows an idea that has been published by Grüne et al. (2010) for single-loop systems and extends it to decentralized control. Based on the separation of the control problem (ultimate boundedness of the closed-loop system) into two problems, namely

1. steering the state from an initial state into a target region and
2. keeping the state in the target region in spite of exogenous disturbances or interconnections with other subsystems,

the global and the local approach are tailored to the respective task. Hence, the combination of both approaches leads to a new method for the decentralized stabilization and disturbance attenuation of interconnected systems. Although the global and the local approach use different models (nonlinear vs. linear) and follow different ideas (stabilization vs. disturbance attenuation), they are similar in the sense that event-based controllers for the isolated subsystems are designed and their robustness with respect to the

interactions of the subsystems are proved by small-gain theorems.

Outline of the paper. The general control problem is formally stated in Sec. 2. The global approach and the local approach are explained in Sections 3 and 4, respectively. The combination of both control methods is described in Sec. 5. Sections 6 and 7 introduce the continuous flow process, shows the implementation of the decentralized event-based controllers in MATLAB/Simulink and gives the experimental results and their discussions.

Nomenclature. $\mathbb{R}$ and $\mathbb{R}_+$ denote the set of real numbers and nonnegative real numbers, respectively, and $\overline{B}_1(0)$ denotes the closed unit ball. For a scalar s, $|s|$ denotes the absolute value. For a vector $\boldsymbol{v} \in \mathbb{R}^n$ or a matrix $\boldsymbol{M} \in \mathbb{R}^{m\times n}$ the $|\cdot|$-operator applies to every element. A comparison between two vectors $\boldsymbol{v}, \tilde{\boldsymbol{v}} \in \mathbb{R}^n$ holds element-wise, like $\boldsymbol{v} \leq \tilde{\boldsymbol{v}}$ amounts to $v_i \leq \tilde{v}_i$ for all $i = 1, \ldots, n$, where v_i and $\tilde{v}_i$ denote the i-th element of the vectors $\boldsymbol{v}$ and $\tilde{\boldsymbol{v}}$, respectively. For a real square matrix $\boldsymbol{M} \in \mathbb{R}^{n\times n}$, $\lambda_{\mathrm{P}}(\boldsymbol{M})$ denotes its Perron root (largest eigenvalue of $\boldsymbol{M}$). A block diagonal matrix with the matrices $\boldsymbol{A}_i$ for $i = 1, \ldots, N$ on the main diagonal is represented by $\boldsymbol{A} = \operatorname{diag}(\boldsymbol{A}_i)$. $\boldsymbol{M}^+$ denotes the pseudoinverse of a matrix $\boldsymbol{M} \in \mathbb{R}^{m\times n}$ that is determines according to

$$\boldsymbol{M}^+ = (\boldsymbol{M}^\top \boldsymbol{M})^{-1} \boldsymbol{M}^\top,$$

where $\boldsymbol{M}^\top \in \mathbb{R}^{n\times m}$ represents the transpose of $\boldsymbol{M}$. The asterisk $*$ symbolizes the convolution-operator, e.g.

$$\boldsymbol{G} * \boldsymbol{u} = \int_0^t \boldsymbol{G}(t-\tau)\boldsymbol{u}(\tau)\mathrm{d}\tau.$$

For a signal $\boldsymbol{x} : \mathbb{R}_+ \to \mathbb{R}^n$, the limit from above at time $t \in \mathbb{R}_+$ is denotes by $\boldsymbol{x}(t^+) = \lim_{s \downarrow t} \boldsymbol{x}(s)$. We introduce the following sets of comparison functions: $\mathcal{K} = \{\gamma : \mathbb{R}_+ \to \mathbb{R}_+, \gamma \text{ is continuous, strictly increasing, and } \gamma(0) = 0\}$, $\mathcal{K}_\infty = \{\gamma \in \mathcal{K} : \gamma \text{ is unbounded}\}$ and $\mathcal{KL} = \{\beta : \mathbb{R}_+ \times \mathbb{R}_+ \to \mathbb{R}_+ : \beta(\cdot, t) \in \mathcal{K}$ and for each fixed $s \geq 0$ it is decreasing to zero as $t \to \infty\}$.

2. Problem formulation

2.1. Structure of the event-based control system

The structure of the event-based control system investigated in this paper is illustrated in Fig. 1. The overall plant Σ is composed of N physically interconnected subsystems Σ_i, $(i = 1, \ldots, N)$. The subsystem Σ_i is controlled by an event-based controller consisting of the control input generator C_i and the event generator E_i. The event-based control method that is proposed in this paper is decentralized in two senses:

1. The event times t_k at which a feedback communication is invoked are determined by the event generators E_i based on locally available information only and
2. the control input generator C_i produces the control input for subsystem Σ_i using only information that is received at the event times from the event generator E_i.

The latter implies the decentralized communication structure as shown in Fig. 1, where the information is transmitted from the event generator E_i to the corresponding control input generator C_i, but to no other component. Note that this communication structure opens the possibility to realize the

feedback communication of the respective control loops over various networks. A communication from E_i to C_i is only invoked at the event times t_k, which is expressed by the dashed line in Fig. 1. The solid lines represent continuous information links. In this paper, the information transmission over the communication network is assumed to occur instantaneously and without delays or packet losses.

2.2. Plant model

The overall plant is composed of N subsystems and is described by the nonlinear state-space model

$$\Sigma : \begin{cases} \dot{\boldsymbol{x}}_1(t) = \boldsymbol{f}_1(\boldsymbol{x}_1(t), \ldots, \boldsymbol{x}_N(t), \boldsymbol{u}_1(t), \boldsymbol{d}_1(t)) \\ \qquad\qquad \vdots \\ \dot{\boldsymbol{x}}_N(t) = \boldsymbol{f}_N(\boldsymbol{x}_1(t), \ldots, \boldsymbol{x}_N(t), \boldsymbol{u}_N(t), \boldsymbol{d}_N(t)) \end{cases} \tag{1}$$

with initial conditions $\boldsymbol{x}_i(0) = \boldsymbol{x}_{0i}$ for all $i \in \mathcal{N} := \{1, \ldots, N\}$. In (1), $\boldsymbol{x}_i \in \mathcal{X}_i \subset \mathbb{R}^{n_i}$, $\boldsymbol{u}_i \in \mathcal{U}_i \subset \mathbb{R}^{m_i}$ and $\boldsymbol{d}_i \in \mathcal{D}_i \subset \mathbb{R}^{w_i}$ are the state, the control input and the disturbance of the i-th subsystem denoted by Σ_i. In the following,

$$\mathcal{D}_i := \left\{ \boldsymbol{d}_i \mid |\boldsymbol{d}_i| \leq \bar{\boldsymbol{d}}_i \right\}, \tag{2}$$

where the vector $\bar{\boldsymbol{d}}_i$ element-wise denotes the maximum magnitude of the disturbance vector $\boldsymbol{d}_i(t)$. The state, the control input and the disturbance of the overall plant Σ are represented by

$$\begin{aligned} \boldsymbol{x}(t) &= \left(\boldsymbol{x}_1^\top(t), \ldots, \boldsymbol{x}_N^\top(t)\right)^\top \\ \boldsymbol{u}(t) &= \left(\boldsymbol{u}_1^\top(t), \ldots, \boldsymbol{u}_N^\top(t)\right)^\top \\ \boldsymbol{d}(t) &= \left(\boldsymbol{d}_1^\top(t), \ldots, \boldsymbol{d}_N^\top(t)\right)^\top. \end{aligned}$$

The full state space, set of controls and set of disturbances are denoted by $\mathcal{X} = \mathcal{X}_1 \times \ldots \times \mathcal{X}_N$, $\mathcal{U} = \mathcal{U}_1 \times \ldots \times \mathcal{U}_N$ and $\mathcal{D} = \mathcal{D}_1 \times \ldots \times \mathcal{D}_N$, respectively.

2.3. Control aim

The control aim is formulated in terms of ultimate boundedness:

Definition 1 (Ultimate boundedness). *The solution $\boldsymbol{x}(t)$ of (1) is called ultimately bounded (UB) to the set $\mathcal{A}$ if for each initial condition $\boldsymbol{x}_0 \in \mathcal{X}$ there exists a time $T(\boldsymbol{x}_0) > 0$ such that*

$$\boldsymbol{x}(t) \in \mathcal{A}, \quad \forall\ t \geq T(\boldsymbol{x}_0) \tag{3}$$

holds for all admissible disturbances $\boldsymbol{d}(t) \in \mathcal{D}$. The system (1) is said to be ultimately bounded if its state $\boldsymbol{x}(t)$ is UB.

Consider that the system Σ as in (1) and a target set $\mathcal{A} = \mathcal{A}_1 \times \ldots \times \mathcal{A}_N$ are given, where $\mathcal{A}_i \subset \mathcal{X}_i$ denotes the target set for the subsystem Σ_i. The aim of the first part of this paper is to develop a method for the design of decentralized event-based state-feedback controllers $\boldsymbol{K}_i : \mathcal{X}_i \to \mathcal{U}_i$ that render the closed-loop system ultimately bounded to the set $\mathcal{A}$.

2.4. A global and a local approach

The proposed event-based control approach follows an idea that has been presented by Grüne et al. (2010) for single-loop event-based control systems. As illustrated in Fig. 2, the problem of finding the decentralized event-based controllers $\boldsymbol{K}_i$ that render the closed-loop system ultimately bounded is subdivided into a global problem and a local problem, which are solved by two complementary approaches:

1. The *global event-based control approach* drives the state $\boldsymbol{x}_i(t)$ of each subsystem Σ_i from the initial state $\boldsymbol{x}_{0i}$ into the target set $\mathcal{A}_i$, while taking possible constraints on the states or on the control inputs into account.
2. The *local event-based control approach* makes the set $\mathcal{A}_i$ for each Σ_i robustly positive invariant, i.e. once the state $\boldsymbol{x}_i(t)$ enters $\mathcal{A}_i$ it is kept within this set in spite of exogenous disturbances $\boldsymbol{d}_i(t)$ and interconnections to other subsystems.

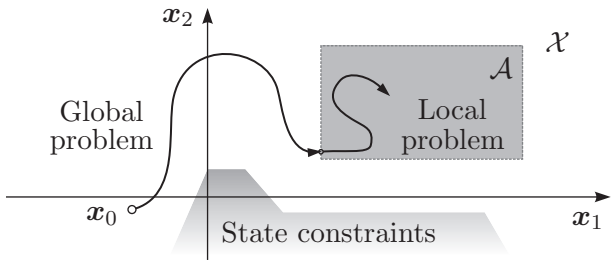

Figure 2: The global and the local problem

Global approach – Nonlinear control. Section 3 proposes an optimization-based method for the design of a decentralized event-based controller which accomplishes the transition of the state $\boldsymbol{x}(t)$ of the nonlinear system Σ given in (1) from an initial state $\boldsymbol{x}_0$ to the target set $\mathcal{A}$. The state-feedback law for subsystem Σ_i uses quantized information $[\boldsymbol{x}_i(t)]$ about the state $\boldsymbol{x}_i(t)$ only. This quantization coarsely partitions the state space $\mathcal{X}_i$ into a grid of boxes in each of which the control input $\boldsymbol{u}_i(t)$ is held constant. The event-based character of the controller lies in updating the control input $\boldsymbol{u}_i(t)$ only after the state $\boldsymbol{x}_i(t)$ has crossed the boundary of a box, which is detected by the

event generator E_i. The control input generator C_i is realized as a look-up table that can be computed offline.

Local approach – Linear control. For the local approach, the target set $\mathcal{A}$ is considered as a bounded surrounding of the operating point $\bar{\boldsymbol{x}}$ in which the system Σ is described by a linearized model with sufficient accuracy. The control input generator C_i determines the control input $\boldsymbol{u}_i(t)$ using a linear model $\Sigma_{\mathrm{s}i}$ of the subsystem Σ_i with a continuous state-feedback controller. The event generator E_i monitors the deviation between the actual subsystem state $\boldsymbol{x}_i(t)$ and the state $\boldsymbol{x}_{\mathrm{s}i}(t)$ of the model $\Sigma_{\mathrm{s}i}$ used for the generation of the control input $\boldsymbol{u}_i(t)$ and it triggers an event whenever this deviation exceeds a defined threshold.

Switching from the global to the local approach. The control input generator C_i as well as the event generator E_i include the respective components which are designed according to the global and the local approach. C_i and E_i work as specified by the global approach as long as $\boldsymbol{x}_i(t) \notin \mathcal{A}_i$. T_i denotes the time instant at which $\boldsymbol{x}_i(T_i)$ enters the set $\mathcal{A}_i$. At time $t = T_i$, both C_i and E_i switch their functionality and proceed with working according to the local approach and, hence, the state $\boldsymbol{x}_i(t)$ is maintained within the set $\mathcal{A}_i$ for all $t \geq T_i$.

3. The global approach

3.1. Main idea

In this section the problem of optimally controlling a nonlinear interconnected system to a desired target set $\mathcal{A}$ by means of a quantized state-

feedback law is considered. We utilize the structure of the interconnected system by separately deriving a feedback law for each subsystem Σ_i.

For the calculation of an event-based robustly stabilizing feedback law for each subsystem we use a set oriented approach which has been previously proposed for systems without perturbations in Grüne & Müller (2009), Grüne et al. (2010). As this approach yields only practical stability, we will utilize practical versions of all stability properties involved. For simplicity of exposition, throughout this section we assume that the target set $\mathcal{A}$ contains a neighborhood of the origin.

We sample the nonlinear state-space model (1) to obtain a discrete-time representation of the continuous-time sampled-data system

$$\begin{aligned}\Sigma : \boldsymbol{x}(k+1) &= \begin{cases} \boldsymbol{x}_1(k+1) = \boldsymbol{f}_1(\boldsymbol{x}_1(k), \ldots, \boldsymbol{x}_N(k), \boldsymbol{u}_1(k), \boldsymbol{d}_1(k)) \\ \qquad\qquad \vdots \\ \boldsymbol{x}_N(k+1) = \boldsymbol{f}_N(\boldsymbol{x}_1(k), \ldots, \boldsymbol{x}_N(k), \boldsymbol{u}_N(k), \boldsymbol{d}_N(k)) \end{cases} \\ &= \boldsymbol{f}(\boldsymbol{x}(k), \boldsymbol{u}(k), \boldsymbol{d}(k)),\end{aligned} \tag{4}$$

$k = 0, 1, \ldots$, with initial conditions $\boldsymbol{x}_i(0) = \boldsymbol{x}_{0i}$ for all $i = 1, \ldots, N$, where $\boldsymbol{x}_i \in \mathcal{X}_i \subset \mathbb{R}^{n_i}$, $\boldsymbol{u}_i \in \mathcal{U}_i \subset \mathbb{R}^{m_i}$ and $\boldsymbol{d}_i \in \mathcal{D}_i \subset \mathbb{R}^{w_i}$. Infinite sequences of control and perturbation are denoted by $\underline{\boldsymbol{u}} = (\boldsymbol{u}(0), \boldsymbol{u}(1), \ldots) \in \mathcal{U}^{\mathbb{N}_0}$ and $\underline{\boldsymbol{d}} = (\boldsymbol{d}(0), \boldsymbol{d}(1), \ldots) \in \mathcal{D}^{\mathbb{N}_0}$.

3.2. Small gain approach

We want to construct a decentralized static state feedback controller $\boldsymbol{u}_{\mathcal{P}}$, such that the closed loop system

$$\boldsymbol{x}(k+1) = \boldsymbol{f}(\boldsymbol{x}(k), \boldsymbol{u}_{\mathcal{P}}(\boldsymbol{x}(k)), \underline{\boldsymbol{d}}(k)) =: \boldsymbol{h}(\boldsymbol{x}(k), \underline{\boldsymbol{d}}(k)) \tag{5}$$

is rendered input-to-state practically stable in the following sense

Definition 2. *System* (5) *is called input-to-state practically stable (ISpS) with respect to* $\delta, \Delta_d \in \mathbb{R}_{\geq 0}$ *on a set* $\mathcal{Y} \subset \mathcal{X}$ *if there exist* $\beta \in \mathcal{KL}$ *and* $\gamma \in \mathcal{K}$*, such that the solutions of the system satisfy*

$$\|\boldsymbol{x}(k)\| \leq \max\{\beta(\|\boldsymbol{x}_0\|, k), \gamma(\|\underline{\boldsymbol{d}}\|_\infty), \delta\}, \tag{6}$$

for all $\boldsymbol{x}_0 \in \mathcal{Y}$*, all* $\underline{\boldsymbol{d}} \in \mathcal{D}^{\mathbb{N}_0}$ *with* $\|\underline{\boldsymbol{d}}\|_\infty \leq \Delta_d$ *and all* $k \in \mathbb{N}_0$*.*

Since we assumed that the target set $\mathcal{A}$ contains a neighborhood of the origin, this property ensures ultimated boundedness w.r.t. $\mathcal{A}$ provided δ and $\|\boldsymbol{d}\|$ are sufficiently small. If (6) holds with $\gamma = 0$ the system is called uniformly practically asymptotically stable.

The idea we pursue for the decentralized design is to derive an ISpS-controller for each subsystem Σ_i, where the input from the other subsystems is considered as an additional perturbation. Then, stability of the overall system can be ensured via a small-gain argument. The central tool for this purpose are ISpS Lyapunov functions since ISpS can be characterized through them. Here we provide the definition of an ISpS Lyapunov function for the subsystems.

Definition 3. *A continuous function* $\boldsymbol{V}_i : \mathcal{X}_i \to \mathbb{R}_{\geq 0}$ *is called ISpS Lyapunov function for the i-th subsystem* Σ_i *of* (4) *on a sublevel set* $\mathcal{Y}_i = \{\boldsymbol{x}_i \in \mathcal{X}_i \,|\, V_i(\boldsymbol{x}_i) \leq \ell_i\}$ *for some* $\ell_i > 0$ *with respect to a Lyapunov target set* $\mathcal{A}_i^V \subset \mathcal{Y}_i$*, if there exist functions* $\underline{\alpha}_i, \overline{\alpha}_i \in \mathcal{K}_\infty$*,* $\alpha_i, \mu_{ij} \in \mathcal{K} \cup \{0\}$*,* $\mu_i \in \mathcal{K}$*, a value* $\overline{w} \in \mathbb{R}_{>0}$ *such that for all* $\boldsymbol{x} \in \mathcal{Y}_i \backslash \mathcal{A}_i^V$ *the inequalities and implications*

$$\underline{\alpha}_i(\|\boldsymbol{x}_i\|) \leq V_i(\boldsymbol{x}_i) \leq \overline{\alpha}_i(\|\boldsymbol{x}_i\|) \tag{7}$$

and

$$V_i(\boldsymbol{x}_i) \geq \max\{\max_j\{\mu_{ij}(\|\boldsymbol{x}_j\|_\infty)\}, \mu_i(\|\boldsymbol{d}\|_\infty)\}$$
$$\Rightarrow\ V_i(\boldsymbol{x}_i(k+1)) - V_i(\boldsymbol{x}_i(k)) \leq -\alpha_i(|\boldsymbol{x}_i|) \qquad (8)$$

hold for all $\boldsymbol{w} \in \mathcal{V}$ *with* $\|\boldsymbol{w}\| \leq \overline{w}$.

The functions μ_{ij} and μ_i are called Lyapunov gains. By definition we set $\mu_{ii} \equiv 0$. Note that the Lyapunov target $\mathcal{A}^V$ will in general be smaller than the target set $\mathcal{A}$ since no invariance of $\mathcal{A}^V$ can be guaranteed, for details see the discussion after Theorem 1.

From small-gain theorems (see Dashkovskiy et al. (2010)) it is known that, if the gains μ_{ij} are sufficiently small, a Lyapunov function V for the overall system exists. While this result is currently only proved for continuous time systems, our experiments indicate that it also holds in an event based setting.

The following theorem states that the existence of an ISpS Lyapunov function implies that the system is ISpS. This is fairly straightforward if all data is continuous. However, since in our approach the ISpS-Lyapunov function and the resulting feedback for the subsystems may not be continuous, we introduce the following conditions, cf. (Grüne & Sigurani, 2013, Assumptions 7 and 8).

Assumption 1. *The map* $\boldsymbol{f} : \mathcal{X}\times\mathcal{U}\times\mathcal{V} \to \mathbb{R}^n$ *in* (4) *is uniformly continuous in* $\boldsymbol{w} = 0$ *in the following sense: there exists a* $\gamma_d \in \mathcal{K}_\infty$*, such that for all* $\boldsymbol{x} \in \mathcal{X}$*,* $\boldsymbol{u} \in \mathcal{U}$ *and* $\boldsymbol{d} \in \mathcal{D}$

$$\|\boldsymbol{f}(\boldsymbol{x}, \boldsymbol{u}, \boldsymbol{d}) - \boldsymbol{f}(\boldsymbol{x}, \boldsymbol{u}, \boldsymbol{0})\| \leq \gamma_d(\|\boldsymbol{d}\|). \qquad (9)$$

Assumption 2. *The map $\boldsymbol{h} : \mathcal{X} \times \mathcal{D} \to \mathbb{R}^n$ in (5) is bounded for $\boldsymbol{d} = \boldsymbol{0}$ on $\mathcal{A}$ in the following sense: there exists $\gamma_x \in \mathcal{K}_\infty$ such that for all sufficiently small sets $\mathcal{A} \subset \mathcal{X}$ with $\boldsymbol{0} \in \mathcal{A}$ and each $\boldsymbol{x} \in \mathcal{A}$ we have*

$$\|\boldsymbol{f}(\boldsymbol{x}, \boldsymbol{u}_{\mathcal{P}}(\boldsymbol{x}), \boldsymbol{0})\| \leq \gamma_x(\|\boldsymbol{x}\|). \tag{10}$$

Now we can state the relation between the existence of an ISpS Lyapunov function and the ISpS property of the system, cf. (Grüne & Sigurani, 2013, Theorem 10).

Theorem 1. *Consider system (5) satisfying Assumptions 1 and 2 and assume that the system admits an ISpS Lyapunov function V. Then the system is ISpS on $\mathcal{Y}$, with $\Delta_d \to \infty$ as $\ell \to \infty$ and $\delta \to 0$ as $\sup_{x \in \mathcal{A}^V} \|\boldsymbol{x}\| \to 0$, provided $\delta \leq \underline{\alpha}^{-1}(\ell)$ holds.*

The relation between the size of the Lyapunov target $\mathcal{A}^V$ and the practical stability parameter δ is made more precise in (Grüne & Sigurani, 2013, Theorem 10). However, for our purpose the decisive property is that $\delta \to 0$ as $\sup_{x \in \mathcal{A}^V} \|\boldsymbol{x}\| \to 0$. Since the target $\mathcal{A}$ contains a neighborhood of the origin, this convergence implies ultimate boundedness w.r.t. $\mathcal{A}$ for vanishing perturbation if δ and thus $\mathcal{A}^V$ are sufficiently small. In practice, given $\mathcal{A}$ one can determine an appropriate $\mathcal{A}^V$ by numerical simulations.

3.3. Conversion to a robust stabilization problem

The goal of this section is to design an ISpS-controller for each subsystem Σ_i. Recall that we consider the influence of the other states $\boldsymbol{x}_j, j \neq i \in 1, \ldots, N$, as perturbations and thus extend the perturbation of Σ_i to $\boldsymbol{v}_i = (\boldsymbol{x}_j \ \ldots \ \boldsymbol{x}_{N-1} \ \boldsymbol{d}_i) \in \mathcal{V}_i = \mathcal{X}_j \times \ldots \times \mathcal{X}_{N-1} \times \mathcal{D}_i, j \neq i \in 1, \ldots, N$. Since this

section only deals with a single subsystem, for simplicity we will omit the indices i in the sequel, i.e., we write the subsystem as

$$\boldsymbol{x}(k+1) = \boldsymbol{f}(\boldsymbol{x}(k), \underline{\boldsymbol{u}}(k), \underline{\boldsymbol{v}}(k)). \tag{11}$$

In order to design an ISpS controller for (11), we follow the approach in Grüne & Sigurani (2013), which in turn is based on ideas from Jiang & Wang (2001). This approach uses that system (5) is ISpS if and only if it is practically robustly stable. Practical robust stability means that there exists $\boldsymbol{e} : \mathcal{X} \times \mathcal{V} \to \mathcal{V}$ and $\eta \in \mathcal{K}_\infty$ such that the system

$$\boldsymbol{x}(k+1) = \boldsymbol{f}(\boldsymbol{x}(k), \boldsymbol{u}_{\mathcal{P}}(\boldsymbol{x}(k)), \boldsymbol{e}(\boldsymbol{x}(k), \underline{\tilde{\boldsymbol{v}}}(k))) \tag{12}$$

with $\widetilde{\mathcal{V}} = \overline{B}_1(0)$ is uniformly practically asymptotically stable, where $\boldsymbol{e}$ is such that for each $\boldsymbol{v} \in \mathcal{V}$ with $\|\boldsymbol{v}\| \leq \eta(\|\boldsymbol{x}\|)$ there exists $\tilde{\boldsymbol{v}} \in \widetilde{\mathcal{V}}$ with $\boldsymbol{e}(\boldsymbol{x}, \tilde{\boldsymbol{v}}) = \boldsymbol{v}$.

3.4. Solution of the robust stabilization problem

In order to construct a controller rendering the system uniformly practically asymptotically stable we employ the dynamic game approach from Grüne & Junge (2007) which in turn relies on ideas from Grüne & Junge (2008), Junge & Osinga (2004). This approach introduces a discretization of the state space $\mathcal{X}$ using a finite partition $\mathcal{P}$ of boxes P. Below, we describe the discrete time version of this approach. Its event-based extension, as introduced and discussed in Grüne & Müller (2009) and Grüne et al. (2010), is straightforward using the observation that the control value only changes when the state moves from one partition element P to another. Hence, an event is triggered whenever the state leaves a partition element. This event

based implementation is used in the experiments in Section 7.

Let a target set $\mathcal{A}^V$ be given which contains a neighborhood of the origin. Note that $\mathcal{A}_i^V$ is the target set for the state of the i-th subsystem. We select a stage cost $g : \mathcal{X} \times \mathcal{U} \to \mathbb{R}$ which penalizes the distance to the origin and define the accumulated cost as

$$J(\boldsymbol{x}_0, \underline{\boldsymbol{u}}, \underline{\boldsymbol{v}}) := \sum_{k=0}^{k(\mathcal{A}^V, \boldsymbol{x}_0, \underline{\boldsymbol{u}}, \underline{\boldsymbol{v}})} g(\boldsymbol{x}(k, \boldsymbol{x}_0, \underline{\boldsymbol{u}}, \underline{\boldsymbol{v}}), \boldsymbol{u}(k)),$$

where $k(\mathcal{A}^V, \boldsymbol{x}_0, \underline{\boldsymbol{u}}, \underline{\boldsymbol{v}})$ denotes the smallest k for which $\boldsymbol{x}(k, \boldsymbol{x}_0, \underline{\boldsymbol{u}}, \underline{\boldsymbol{v}}) \in \mathcal{A}^V$ holds.

The computation of V is performed by a graph theoretic approximation of the dynamics of the system on the partition $\mathcal{P}$. Since the model includes both control and perturbation the resulting graph takes the form of a hypergraph. The computation of V can then be carried out by solving a generalized min-max shortest path problem on this hypergraph. This yields an approximation $V_{\mathcal{P}}$ of V which is constant on each element P of the partition $\mathcal{P}$. An approximation $\boldsymbol{u}_{\mathcal{P}}$ of the optimal controller is obtained through the dynamic programming principle

$$\boldsymbol{u}_{\mathcal{P}}(\boldsymbol{x}) := \operatorname*{argmin}_{\boldsymbol{u} \in U} \left\{ g(\boldsymbol{x}, \boldsymbol{u}) + \sup_{\boldsymbol{x}' \in \boldsymbol{f}(\boldsymbol{x}, \boldsymbol{u}, W)} V_{\mathcal{P}}(\boldsymbol{x}') \right\}. \tag{13}$$

This controller is defined on the stabilizable set w.r.t. $V_{\mathcal{P}}$ given by $S_{\mathcal{P}} := \{\boldsymbol{x} \in \mathcal{X} \mid V_{\mathcal{P}}(\boldsymbol{x}) < \infty\}$. For details we refer to Grüne & Junge (2007). Note that neither $V_{\mathcal{P}}$ nor $\boldsymbol{u}_{\mathcal{P}}$ are continuous, hence we introduced Assumptions 1 and 2.

The following theorem in (Grüne & Sigurani, 2013, Theorem 12) summarizes the derivation outlined in this section.

Theorem 2. *Consider the subsystem* (11) *satisfying Assumptions 1 and 2 and let the function* $V_{\mathcal{P}}$ *denote the approximate optimal value function constructed according to the algorithm presented in Grüne & Junge (2007) on a given partition* $\mathcal{P}$ *and target* $\mathcal{A}^V$ *for system* (12). *Denote the corresponding feedback by* $\boldsymbol{u}_{\mathcal{P}}$. *Let* $\ell \leq \max_{\boldsymbol{s}\in S_{\mathcal{P}}} V_{\mathcal{P}}(\boldsymbol{s})$ *and let* $\underline{\alpha}, \overline{\alpha} \in \mathcal{K}_\infty$ *denote functions such that* (7) *holds on* $\mathcal{Y} = \{\boldsymbol{x} \in \mathcal{X} \mid V_{\mathcal{P}}(\boldsymbol{x}) \leq \ell\}$.
Then the system is ISpS on $\mathcal{Y}$, *with* $\Delta_d \to \infty$ *as* $\ell \to \infty$ *and* $\delta \to 0$ *as* $\sup_{x\in\mathcal{A}^V} \|x\| \to 0$, *provided* $\delta \leq \underline{\alpha}^{-1}(\ell)$ *holds.*

We can thus use the proposed algorithm to compute the feedback $\boldsymbol{u}_{i,\mathcal{P}}$ for the subsystem (11) for $i = 1, \ldots .N$. According to Theorem 2, the feedback $\boldsymbol{u}_{\mathcal{P}}(\boldsymbol{x}) = (\boldsymbol{u}_{1,\mathcal{P}}(\boldsymbol{x}_1), \ldots, \boldsymbol{u}_{N,\mathcal{P}}(\boldsymbol{x}_N))$ will then also render system (5) ISpS, provided the gains are sufficiently small.

4. The local approach

This section presents a decentralized event-based state-feedback approach which, once the state $\boldsymbol{x}_i(t)$ of subsystem Σ_i has entered the target set $\mathcal{A}_i$ at time T_i, ensures that $\boldsymbol{x}_i(t) \in \mathcal{A}_i$ holds for $t \geq T_i$ in spite of disturbances $\boldsymbol{d}_i(t)$ and of the interconnections to the remaining subsystems. For the overall system, the relation $\boldsymbol{x}(t) \in \mathcal{A} \Leftrightarrow \boldsymbol{x}_i(t) \in \mathcal{A}_i$, for all $i \in \mathcal{N}$ holds (cf. Fig. 3).

4.1. Models

The target set $\mathcal{A}_i$ is a surrounding of the operating point $\bar{\boldsymbol{x}}_i$ of Σ_i, in which Σ_i is described for $t \geq T_i$ by the linear state-space model

$$\Sigma_i : \begin{cases} \dot{\boldsymbol{x}}_i(t) = \boldsymbol{A}_i \boldsymbol{x}_i(t) + \boldsymbol{B}_i \boldsymbol{u}_i(t) + \boldsymbol{E}_i \boldsymbol{d}_i(t) + \boldsymbol{E}_{\mathrm{s}i} \boldsymbol{s}_i(t) \\ \boldsymbol{x}_i(T_i) = \boldsymbol{x}_{\mathrm{T}i} \\ \boldsymbol{z}_i(t) = \boldsymbol{C}_{zi} \boldsymbol{x}_i(t), \end{cases} \tag{14}$$

where $\boldsymbol{s}_i \in \mathbb{R}^{p_i}$ and $\boldsymbol{z}_i \in \mathbb{R}^{q_i}$ denote the coupling input and coupling output, respectively. Σ_i is interconnected with the remaining subsystems according to the relation

$$\boldsymbol{s}_i(t) = \sum_{j=1}^{N} \boldsymbol{L}_{ij} \boldsymbol{z}_j(t), \tag{15}$$

where $\boldsymbol{L}_{ii} = \boldsymbol{0}$ holds for all $i \in \mathcal{N}$ by assumption. The control input generator C_i and the event generator E_i for Σ_i are designed by using the method of Lunze & Lehmann (2010), which is applied here for the isolated subsystems

$$\dot{\boldsymbol{x}}_i(t) = \boldsymbol{A}_i \boldsymbol{x}_i(t) + \boldsymbol{B}_i \boldsymbol{u}_i(t) + \boldsymbol{E}_i \boldsymbol{d}_i(t), \quad \boldsymbol{x}_i(T_i) = \boldsymbol{x}_{\mathrm{T}i}, \quad i \in \mathcal{N} \tag{16}$$

and leads to the components explained in the next sections.

4.2. Components of the event-based control loops

Control input generators C_i. In the interval $t \in [t_{k_i}, t_{k_i+1})$, the control input generators C_i are represented by the model

$$C_i : \begin{cases} \Sigma_{\mathrm{s}i} : \begin{cases} \dot{\boldsymbol{x}}_{\mathrm{s}i}(t) = \bar{\boldsymbol{A}}_i \boldsymbol{x}_{\mathrm{s}i}(t) + \boldsymbol{E}_i \hat{\boldsymbol{d}}_i(t_{k_i}) \\ \boldsymbol{x}_{\mathrm{s}i}(t_{k_i}^+) = \boldsymbol{x}_i(t_{k_i}) \end{cases} \\ \boldsymbol{u}_i(t) = -\boldsymbol{K}_i \boldsymbol{x}_{\mathrm{s}i}(t) \end{cases} \tag{17}$$

for $i \in \mathcal{N}$, where $\boldsymbol{x}_{\mathrm{s}i} \in \mathbb{R}^{n_i}$ denotes the state and $\hat{\boldsymbol{d}}_i(t_{k_i})$ is a disturbance estimate. This event-based control approach works with any disturbance estimation method that yields bounded estimates $\hat{\boldsymbol{d}}_i(t_{k_i})$, e. g. with the trivial estimation $\hat{\boldsymbol{d}}_i(t_{k_i}) \equiv \boldsymbol{0}$ for all $k_i \in \mathbb{N}_0$ or with the more sophisticated disturbance estimate presented in Stöcker et al. (2013). In (17), the state-feedback gain $\boldsymbol{K}_i$ is chosen such that the matrix

$$\bar{\boldsymbol{A}}_i := \boldsymbol{A}_i - \boldsymbol{B}_i \boldsymbol{K}_i$$

is Hurwitz.

Event generators E_i. Like the control input generators, the event generators include the model $\Sigma_{\mathrm{s}i}$ defined in (17). In order to determine the event times t_{k_i} ($k_i = 1, 2, \ldots$), E_i monitors the difference state

$$\boldsymbol{x}_{\Delta i}(t) := \boldsymbol{x}_i(t) - \boldsymbol{x}_{\mathrm{s}i}(t)$$

and triggers an event, whenever the condition

$$\big\| |\boldsymbol{x}_{\Delta i}(t)| - \bar{\boldsymbol{e}}_i \big\|_\infty = 0 \tag{18}$$

is satisfied, where $\bar{\boldsymbol{e}}_i \in \mathbb{R}_+^{n_i}$ denotes the event threshold vector. Hence, E_i continuously measures the subsystem state $\boldsymbol{x}_i(t)$ and it determines the event times t_{k_i} using the model

$$E_i : \begin{cases} \Sigma_{\mathrm{s}i} : \begin{cases} \dot{\boldsymbol{x}}_{\mathrm{s}i}(t) = \bar{\boldsymbol{A}}_i \boldsymbol{x}_{\mathrm{s}i}(t) + \boldsymbol{E}_i \hat{\boldsymbol{d}}_i(t_{k_i}) \\ \boldsymbol{x}_{\mathrm{s}i}(t_{k_i}^+) = \boldsymbol{x}_i(t_{k_i}) \end{cases} \\ t_{k_i} := \min\big\{ t > t_{k_i - 1} \;\big|\; \| |\boldsymbol{x}_{\Delta i}(t)| - \bar{\boldsymbol{e}}_i \|_\infty = 0 \big\}. \end{cases} \tag{19}$$

At the event time t_{k_i}, E_i transmits the current subsystem state $\boldsymbol{x}_i(t_{k_i})$ to C_i and this information is used in both components to reset the state $\boldsymbol{x}_{\mathrm{s}i}$ of the model $\Sigma_{\mathrm{s}i}$, which implies $\boldsymbol{x}_{\Delta i}(t_{k_i}^+) = \boldsymbol{0}$ for all event times t_{k_i}, $k_i \in \mathbb{N}_0$.

4.3. Stability analysis

The control input generator C_i and the event generator E_i are designed under the assumption of vanishing interconnections ($\boldsymbol{s}_i(t) = \mathbf{0}$ for all $i \in \mathcal{N}$) and with the aim to ensure the stability of the isolated event-based control loops. This section presents a condition on the interconnection matrix $\boldsymbol{L}$ for which the stability of the isolated event-based control loops implies the stability of the overall control system.

The following theorem summarizes a stability test which has been derived by Stöcker et al. (2013) using the comparison principle (see Lunze (1992)).

Theorem 3 (Stöcker et al. (2013)). *The overall event-based control system that consists of the interconnected subsystems* (14), (15) *and the decentralized event-based controllers* (17), (19) *is ultimately bounded if the condition*

$$\lambda_{\mathrm{P}} \left(\int_0^\infty \bar{\boldsymbol{G}}_{\mathrm{xs}}(t) \bar{\boldsymbol{L}} \bar{\boldsymbol{C}}_{\mathrm{z}} \mathrm{d}t \right) < 1 \tag{20}$$

is satisfied with

$$\bar{\boldsymbol{G}}_{\mathrm{xs}}(t) = \mathrm{diag}\left(\left| \mathrm{e}^{\bar{\boldsymbol{A}}_i t} \boldsymbol{E}_{\mathrm{s}i} \right| \right), \tag{21}$$

$$\bar{\boldsymbol{C}}_{\mathrm{z}} = \mathrm{diag}\left(|\boldsymbol{C}_{\mathrm{z}i}| \right). \tag{22}$$

The matrix

$$\bar{\boldsymbol{L}} = \begin{pmatrix} \mathbf{0} & |\boldsymbol{L}_{12}| & \dots & |\boldsymbol{L}_{1N}| \\ |\boldsymbol{L}_{21}| & \mathbf{0} & \dots & |\boldsymbol{L}_{2N}| \\ \vdots & \vdots & \ddots & \vdots \\ |\boldsymbol{L}_{N1}| & |\boldsymbol{L}_{N2}| & \dots & \mathbf{0} \end{pmatrix} \tag{23}$$

represents a bound on the interconnections among the subsystems.

The stability condition (20) is a small-gain condition requiring the interconnection among the subsystems to be sufficiently weak. Hence, (20) can be used to find a bound on the interconnection up to which the stability of the overall system is guaranteed.

The following result explicitely states a region $\mathcal{B}$ in which the state $\boldsymbol{x}(t)$ of the overall system is maintained by the decentralized event-based controller (17), (19).

Theorem 4 (Stöcker et al. (2013)). *Consider the interconnected subsystems* (14), (15) *together with the decentralized event-based controllers* (17), (19) *and assume that the condition* (20) *is satisfied. The set*

$$\mathcal{B} := \left\{ \boldsymbol{x} = \left(\boldsymbol{x}_1^\top \dots \boldsymbol{x}_N^\top \right)^\top \in \mathbb{R}^n \;\middle|\; \left(|\boldsymbol{x}_1| \dots |\boldsymbol{x}_N| \right)^\top \leq \boldsymbol{b}(\boldsymbol{\varepsilon}, \boldsymbol{\delta}) \right\} \tag{24}$$

is positive invariant for the overall control system (14), (15), (17), (19), *with the ultimate bound*

$$\boldsymbol{b}(\boldsymbol{\varepsilon}, \boldsymbol{\delta}) = \left(\boldsymbol{I}_n - \int_0^\infty \bar{\boldsymbol{G}}_{\mathrm{xs}}(t) \bar{\boldsymbol{L}} \bar{\boldsymbol{C}}_{\mathrm{z}} \mathrm{d}t \right)^{-1} (\boldsymbol{\varepsilon} + \boldsymbol{\delta}) \tag{25}$$

where

$$\boldsymbol{\varepsilon} = \int_0^\infty \operatorname{diag} \left(\left| \mathrm{e}^{\bar{\boldsymbol{A}}_i t} \boldsymbol{B}_i \boldsymbol{K}_i \right| \right) \mathrm{d}t \cdot \begin{pmatrix} \bar{\boldsymbol{e}}_1^\top & \dots & \bar{\boldsymbol{e}}_N^\top \end{pmatrix}^\top, \tag{26}$$

$$\boldsymbol{\delta} = \int_0^\infty \operatorname{diag} \left(\left| \mathrm{e}^{\bar{\boldsymbol{A}}_i t} \boldsymbol{E}_i \right| \right) \mathrm{d}t \cdot \begin{pmatrix} \bar{\boldsymbol{d}}_1^\top & \dots & \bar{\boldsymbol{d}}_N^\top \end{pmatrix}^\top \tag{27}$$

and the matrices $\bar{\boldsymbol{G}}_{\mathrm{xs}}(t)$, $\bar{\boldsymbol{C}}_{\mathrm{z}}$ *and* $\bar{\boldsymbol{L}}$ *are given in* (21)–(23).

The inverse matrix in (25) exists if the condition (20) is satisfied. Theorem 4 shows that the size of the set $\mathcal{B}$ depends upon the disturbance magnitudes $\bar{d}_i$ and the event thresholds $\bar{e}_i$ and that it can be adjusted by appropriately setting the event thresholds $\bar{e}_i$ for all $i \in \mathcal{N}$.

5. Combination of the global and the local approach

This section explains how the global and the local approach are merged in order to obtain an event-based controller that renders the overall system ultimately bounded. For a practical application it is reasonable to combine both approaches, as they are complementary in the following ways:

- For steering the state into the target region, the controller of the global approach must be designed on the basis of the nonlinear plant model (1) which appropriately describes the system behavior within the overall state space and includes possible constraints regarding the set of states and control inputs. Once the state enters the target region, it is sufficient to only consider the system behavior in the neighborhood of the operating point by means of a linearized model (14), (15), as done by the controller of the local approach.

- The quantized state $[\boldsymbol{x}_i(t)]$ provides enough information for the controller of the global approach to drive the state towards the target region. Moreover, the quantization reduces the amount of data for the feedback communication. But for keeping the state within the target region and counteracting exogenous disturbances and interconnections to other systems, the controller of the local approach requires more accurate feedback information about the state $\boldsymbol{x}_i(t)$.

The overall event-based controller combines the two approaches by including in each component the functionalities of both the global and local approach.

Besides the previously defined triggering conditions, all event generators E_i also includes the logic that induces the switching from the global to the

local approach in both components. The switching time for the event-based controller for subsystem Σ_i is given by

$$T_i := \inf\{t \geq 0 \mid \boldsymbol{x}_i(t) \in \mathcal{A}_i\}.$$

At this time, E_i switches the functionality from the global to the local approach and transmits a respective command to the corresponding control input generator C_i. The local approach keeps the state $\boldsymbol{x}_i(t)$ within the target set $\mathcal{A}_i$ for all $t \geq T_i$. Note that the decentralized event-based controllers decide locally at which time they switch from the global to the local approach and, thus, the switching occurs asynchronously in time (Fig. 3).

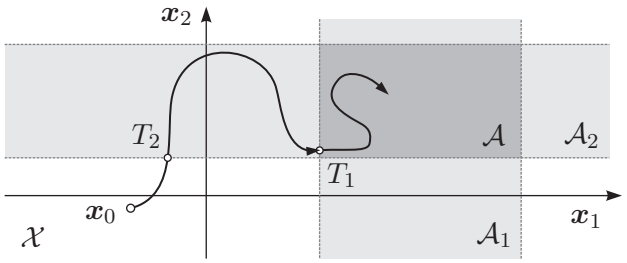

Figure 3: Switching from the global to the local approach

6. Application to a continuous flow process

6.1. Hardware description

The proposed event-based control is tested and evaluated on the pilot plant at the Institute of Automation and Computer Control at Ruhr-University Bochum, Germany (Fig. 4). The plant includes four cylindrical storage tanks, three batch reactors and a buffer tank which are connected over a complex pipe system and it is constructed with standard industrial components including more than 70 sensors and 80 actuators.

Figure 5 illustrates the automation concept for the pilot plant which is subdivided into three layers. On the top layer, the event-based control is implemented on an ordinary personal computer (PC). The functionalities of the control input generators C_i and event generators E_i are realized in MATLAB/Simulink executed with the sampling time $T_\mathrm{s} = 0.3\,\mathrm{s}$. As the sampling time T_s is by a factor of more than 150 smaller than the time constants of the process, the control can be considered to be continuous. The PC is connected over a 100 Mbit/s Ethernet network with the programmable logic controllers (PLCs) on which subordinate controllers and several routines for the plant protection are implemented. On the field level (Sensor/actuator control) the actuator signals are applied and the sensor signals are sampled via the perepherials A to E that are connected over PROFIBUS DP with the PLCs.

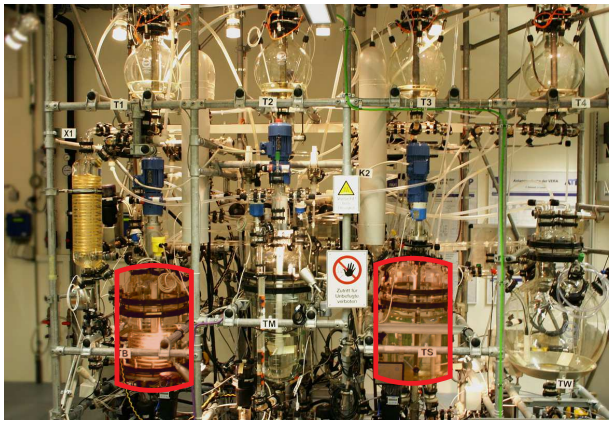

Reactor B Reactor S

Figure 4: Pilot plant. The reactors which are used for the considered process are highlighted.

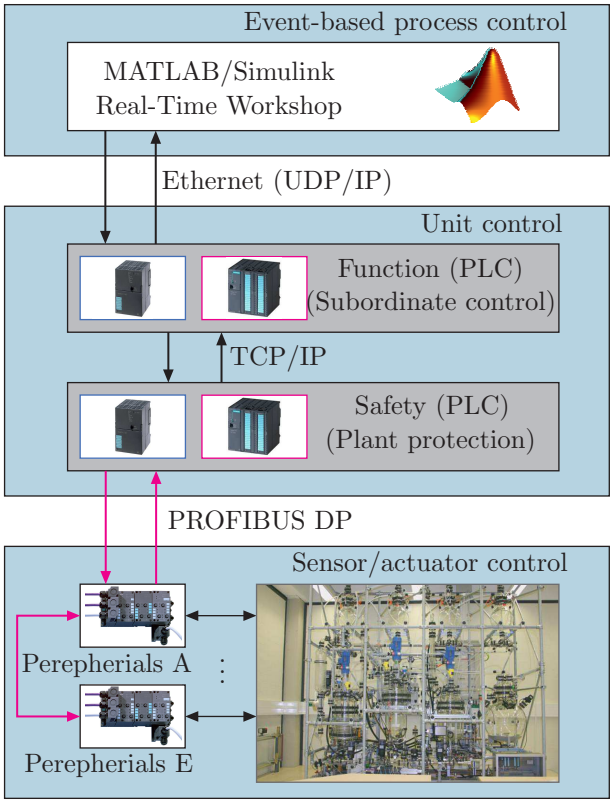

Figure 5: Automation concept for the pilot plant

6.2. Process description

The experimental setup is illustrated in Fig. 6. The main components are the two reactors B and S in which continuous flow processes shall be realized. Reactor B is connected to the storage tank T_1 from where the inflow can be controlled by means of the valve angle u_{T1}. Via the pump PB a part of the outflow is pumped out into the buffer tank TW (and is not used further in the process) while the remaining outflow is conducted to the reactor S. The temperature $\vartheta_B(t)$ of the water in reactor B is influenced by the cooling unit (CU) using the input u_{CU} or by the heating rods that are driven by the signal

d_{H}. The inflow from the storage tank T_3 to the reactor S can be adjusted by means of the opening angle u_{T3}. Reactor S is additionally fed by the fresh water supply (FW) from where the inflow is set by means of the valve angle d_{F}. Equivalently to reactor B, the outflow of reactor S is s! plit and one part is conveyed via the pump PS to TW and the other part is pumped to the reactor B. The temperature $\vartheta_{\mathrm{TS}}(t)$ of the liquid in reactor S can be increased by the heating rods that are controlled by the signal u_{H}.

The two reactors are coupled by the flow from reactor B to reactor S and vice versa, where the coupling strength can be adjusted by means of the valve angles u_{BS} and u_{SB}. The ratio of the volume that is used for the coupling of the systems and the outflow to TW is set by the valve angles u_{BW} and u_{SW}. Both reactor B and reactor S are equipped with sensors that continuously measure the level and the temperature of the contents.

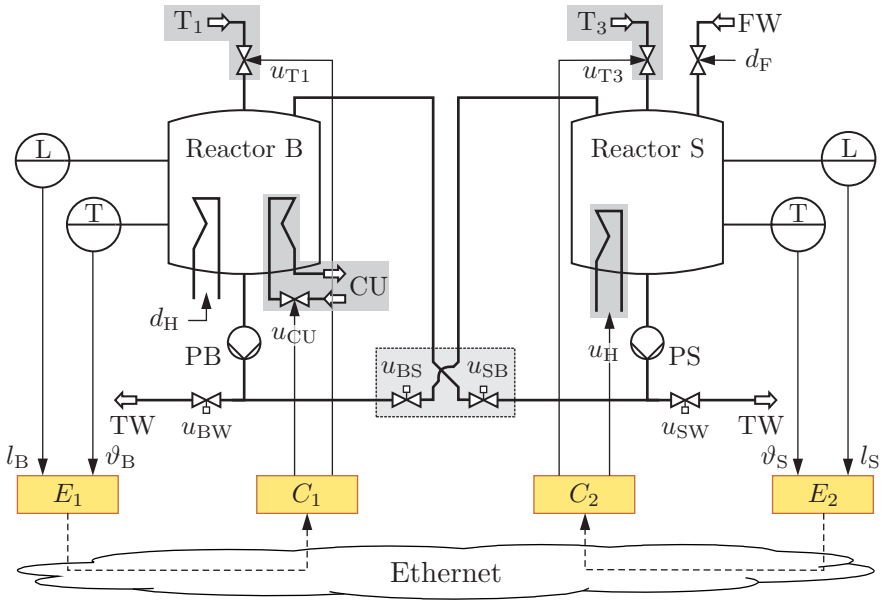

Figure 6: Experimental setup of the continuous flow process

6.3. Plant model

In the following, the behavior of the level and the temperature in reactor B and reactor S are considered as subsystem Σ_1 and Σ_2, respectively. Hence, the states of the subsystems are represented by $\boldsymbol{x}_1(t) = \big(l_{\mathrm{B}}(t)\ \vartheta_{\mathrm{B}}(t)\big)^\top$ and $\boldsymbol{x}_2(t) = \big(l_{\mathrm{S}}(t)\ \vartheta_{\mathrm{S}}(t)\big)^\top$. The continuous flow process is represented by the nonlinear state-space model

$$\begin{aligned}\dot{l}_{\mathrm{B}}(t) = A_{\mathrm{B}}^{-1}\Big(&q_{1\mathrm{B}}(u_{\mathrm{T1}}(t)) + q_{\mathrm{SB}}(l_{\mathrm{S}}(t), u_{\mathrm{SB}}) - q_{\mathrm{BW}}(l_{\mathrm{B}}(t), u_{\mathrm{BW}}) \\ &- q_{\mathrm{BS}}(l_{\mathrm{B}}(t), u_{\mathrm{BS}})\Big) \qquad (28a)\\ \dot{\vartheta}_{\mathrm{B}}(t) = (A_{\mathrm{B}} l_{\mathrm{B}}(t))^{-1}\Big(&q_{1\mathrm{B}}(u_{\mathrm{T1}}(t))(\vartheta_1 - \vartheta_{\mathrm{B}}(t)) + q_{\mathrm{SB}}(l_{\mathrm{S}}(t), u_{\mathrm{SB}})(\vartheta_{\mathrm{S}}(t) - \vartheta_{\mathrm{B}}(t)) \\ &+ q_{\mathrm{C}}(u_{\mathrm{CU}}(t))(\vartheta_{\mathrm{C}} - \vartheta_{\mathrm{B}}(t)) + H_{\mathrm{B}} d_{\mathrm{H}}(t)\Big) \qquad (28b)\\ \dot{l}_{\mathrm{S}}(t) = A_{\mathrm{S}}^{-1}\Big(&q_{3\mathrm{S}}(u_{\mathrm{T3}}(t)) + q_{\mathrm{BS}}(l_{\mathrm{B}}(t), u_{\mathrm{BS}}) - q_{\mathrm{SW}}(l_{\mathrm{S}}(t), u_{\mathrm{SW}}) \\ &- q_{\mathrm{SB}}(l_{\mathrm{S}}(t), u_{\mathrm{SB}}) + q_{\mathrm{FS}}(d_{\mathrm{F}}(t))\Big) \qquad (28c)\\ \dot{\vartheta}_{\mathrm{S}}(t) = (A_{\mathrm{S}} l_{\mathrm{S}}(t))^{-1}\Big(&q_{3\mathrm{S}}(u_{\mathrm{T3}}(t))(\vartheta_3 - \vartheta_{\mathrm{S}}(t)) + q_{\mathrm{BS}}(l_{\mathrm{B}}(t), u_{\mathrm{BS}})(\vartheta_{\mathrm{B}}(t) - \vartheta_{\mathrm{S}}(t)) \\ &+ q_{\mathrm{FS}}(d_{\mathrm{F}}(t))(\vartheta_{\mathrm{F}} - \vartheta_{\mathrm{S}}(t)) + H_{\mathrm{S}} u_{\mathrm{H}}(t)\Big). \qquad (28d)\end{aligned}$$

Here,

$$q_{1\mathrm{B}}(u_{\mathrm{T1}}(t)) = 1.61 \times 10^{-4} \cdot u_{\mathrm{T1}}(t) \qquad (29a)$$

$$q_{3\mathrm{S}}(u_{\mathrm{T3}}(t)) = 1.81 \times 10^{-4} \cdot u_{\mathrm{T3}}(t) \qquad (29b)$$

denote the flows from the storage tanks T_1 and T_3 to the reactors B and S, respectively.

$$q_{\mathrm{C}}(u_{\mathrm{CU}}(t)) = 0.97 \times 10^{-4} \cdot u_{\mathrm{CU}}(t) \qquad (29c)$$

is the flow of the coolant and

$$q_{\mathrm{BS}}(l_{\mathrm{B}}(t), u_{\mathrm{BS}}) = K_{\mathrm{BS}}(u_{\mathrm{BS}})\sqrt{2g l_{\mathrm{B}}(t)} \tag{29d}$$

$$K_{\mathrm{BS}}(u_{\mathrm{BS}}) = 10^{-4} \cdot \begin{cases} 1.02 \cdot u_{\mathrm{BS}}, & 0 \leq u_{\mathrm{BS}} \leq 0.1 \\ 2.13 \cdot u_{\mathrm{BS}} - 0.11, & 0.1 < u_{\mathrm{BS}} \leq 1 \end{cases}$$

$$q_{\mathrm{SB}}(l_{\mathrm{S}}(t), u_{\mathrm{SB}}) = K_{\mathrm{SB}}(u_{\mathrm{SB}})\sqrt{2g l_{\mathrm{S}}(t)} \tag{29e}$$

$$K_{\mathrm{SB}}(u_{\mathrm{SB}}) = 10^{-4} \cdot \begin{cases} 0.90 \cdot u_{\mathrm{SB}}, & 0 \leq u_{\mathrm{SB}} \leq 0.1 \\ 1.68 \cdot u_{\mathrm{SB}} - 0.08, & 0.1 < u_{\mathrm{SB}} \leq 1 \end{cases}$$

denote the flows from reactor B to reactor S and vice versa with the specific valve parameters K_{BS} and K_{SB} (m^3/m). Finally,

$$q_{\mathrm{BW}}(l_{\mathrm{B}}(t), u_{\mathrm{BW}}) = K_{\mathrm{BW}}(u_{\mathrm{TB}})\sqrt{2g l_{\mathrm{B}}(t)} \tag{29f}$$

$$K_{\mathrm{BW}}(u_{\mathrm{BW}}) = 10^{-4} \cdot \begin{cases} 0.96 \cdot u_{\mathrm{TB}}, & 0 \leq u_{\mathrm{BW}} \leq 0.1 \\ 2.01 \cdot u_{\mathrm{TB}} - 0.10, & 0.1 < u_{\mathrm{BW}} \leq 1 \end{cases}$$

$$q_{\mathrm{SW}}(l_{\mathrm{S}}(t), u_{\mathrm{SW}}) = K_{\mathrm{SW}}(u_{\mathrm{SW}})\sqrt{2g l_{\mathrm{S}}(t)} \tag{29g}$$

$$K_{\mathrm{SW}}(u_{\mathrm{SW}}) = 10^{-4} \cdot \begin{cases} 0.79 \cdot u_{\mathrm{SW}}, & 0 \leq u_{\mathrm{SW}} \leq 0.1 \\ 1.42 \cdot u_{\mathrm{SW}} - 0.06, & 0.1 < u_{\mathrm{SW}} \leq 1 \end{cases}$$

denote flows of volume from the reactors B and S into the buffer reactor TW with the specific valve parameters K_{BW} and K_{SW} (m^3/m). All flows have the unit m^3/s. All parameters are listed in Table 1.

Due to technical limitations the subsystem states $\boldsymbol{x}_1 = (l_{\mathrm{B}},\ \vartheta_{\mathrm{B}})^\top$ and

Table 1: Parameters

Parameter	Value	Meaning
A_B	$0.07\ \mathrm{m}^2$	Cross sectional area of tank B
A_S	$0.07\ \mathrm{m}^2$	Cross sectional area of tank S
g	$9.81\ \mathrm{m/s}^2$	Gravitation constant
H_B	$4.8 \times 10^{-3}\ \mathrm{m}^3\mathrm{K/s}$	Heat coefficient of the heating in tank B
H_S	$0.8 \times 10^{-3}\ \mathrm{m}^3\mathrm{K/s}$	Heat coefficient of the heating in tank S
ϑ_1	294.15 K	Temperature of the fluid in tank T_1
ϑ_3	294.15 K	Temperature of the fluid in tank T_3
ϑ_C	282.65 K	Temperature of the coolant
ϑ_F	294.15 K	Temperature of the water supply

$\boldsymbol{x}_2 = (l_\mathrm{S},\ \vartheta_\mathrm{S})^\top$ are restricted to the state space $\mathcal{X} = \mathcal{X}_1 \times \mathcal{X}_2$ with

$$\mathcal{X}_1 = [0.26; 0.40]\ \mathrm{m} \times [285.65; 323.15]\ \mathrm{K} \tag{30a}$$

$$\mathcal{X}_2 = [0.26; 0.40]\ \mathrm{m} \times [293.15; 323.15]\ \mathrm{K}. \tag{30b}$$

The control inputs $\boldsymbol{u}_1 = (u_\mathrm{T1},\ u_\mathrm{CU})^\top$ and $\boldsymbol{u}_2 = (u_\mathrm{T3},\ u_\mathrm{H})^\top$ are limited to the set $\mathcal{U} = \mathcal{U}_1 \times \mathcal{U}_2$ with

$$\mathcal{U}_1 = [0; 1] \times [0; 1]\,, \quad \mathcal{U}_2 = [0; 1] \times [0; 1]\,. \tag{31}$$

Note that the components which are used for the control are highlighted in gray in Fig. 6. The disturbance characteristics are accomplished by means of the heating with disturbance input $d_1(t) = d_\mathrm{H}(t)$ in reactor B and the additional water inflow in reactor S that is set by the valve angle $d_2(t) = d_\mathrm{F}(t)$. The disturbances are considered to be bounded to

$$d_1 \in \mathcal{D}_1 = [0; 0.1]\,, \quad d_2 \in \mathcal{D}_2 = [0; 0.25]\,. \tag{32}$$

6.4. Specification of the control aim

The state $\boldsymbol{x}(t)$ of the overall system shall be steered from a given initial state $\boldsymbol{x}_0 \in \mathcal{X}$ into the target region $\mathcal{A} = \mathcal{A}_1 \times \mathcal{A}_2$ with

$$\mathcal{A}_1 = [0.3; 0.36] \text{ m} \times [291.7; 297.7] \text{ K} \tag{33a}$$

$$\mathcal{A}_2 = [0.31; 0.37] \text{ m} \times [297.2; 303.2] \text{ K} \tag{33b}$$

around the operating point

$$\bar{\boldsymbol{x}}_1 = \begin{pmatrix} \bar{l}_\mathrm{B} \\ \bar{\vartheta}_\mathrm{B} \end{pmatrix} = \begin{pmatrix} 0.33\,\mathrm{m} \\ 294.7\,\mathrm{K} \end{pmatrix}, \quad \bar{\boldsymbol{x}}_2 = \begin{pmatrix} \bar{l}_\mathrm{S} \\ \bar{\vartheta}_\mathrm{S} \end{pmatrix} = \begin{pmatrix} 0.34\,\mathrm{m} \\ 300.2\,\mathrm{K} \end{pmatrix} \tag{34}$$

and maintained in $\mathcal{A}$ for all time in spite of the influence of disturbances given in (32) and interconnections. The interconnections among both subsystems are set by the valve angles u_BS and u_SB which are fixed to

$$u_\mathrm{BS} = 0.19, \quad u_\mathrm{SB} = 0.22 \tag{35}$$

throughout the experiments. Moreover, the choice

$$u_\mathrm{BW} = 0.21, \quad u_\mathrm{SW} = 0.29 \tag{36}$$

defines the outflow from the reactors B and S to the buffer tank TW.

6.5. Decentralized event-based controller resulting from the global approach

The global approach calculates a decentralized event-based controller for each subsystem Σ_1 and Σ_2, utilizing the algorithm described in Section 3. For our experiment we run the algorithm without external disturbances, i.e., we set $d_H = d_F = 0$ and consider only the state of the other subsystem as

disturbance by setting $\boldsymbol{v}_1 = (l_S\ \theta_S)$ and $\boldsymbol{v}_2 = (l_B\ \theta_B)$. The functions

$$\boldsymbol{e}_1(\boldsymbol{x}_1, \tilde{\boldsymbol{v}}_1) = \begin{pmatrix} 0.34 + \sqrt{1.28(l_B - 0.33)^2}\tilde{\boldsymbol{v}}_{11} \\ 300.2 + \sqrt{1053.4(l_B - 0.33)^2 + 0.631338(\theta_B - 294.7)^2}\tilde{\boldsymbol{v}}_{12} \end{pmatrix} \tag{37}$$

and

$$\boldsymbol{e}_2(\boldsymbol{x}_2, \tilde{\boldsymbol{v}}_2) = \begin{pmatrix} 0.33 + \sqrt{0.750312(l_S - 0.34)^2}\tilde{\boldsymbol{v}}_{21} \\ 294.7 + \sqrt{1239.4(l_S - 0.34)^2 + 1.49094(\theta_S - 300.2)^2}\tilde{\boldsymbol{v}}_{12} \end{pmatrix} \tag{38}$$

are used to convert the problem into a robust stabilization problem, thus obtaining system (12) with $\tilde{\boldsymbol{v}}_1 = (\tilde{\boldsymbol{v}}_{11}\ \tilde{\boldsymbol{v}}_{12})^T \in [-1;\ 1]^2$ and $\tilde{\boldsymbol{v}}_2 = (\tilde{\boldsymbol{v}}_{21}\ \tilde{\boldsymbol{v}}_{22})^T \in [-1;\ 1]^2$. The additive terms in $\boldsymbol{e}_1$ and $\boldsymbol{e}_2$ are necessary because in contrast to Section 3 the operating point in our experiment is not located at the origin. Note that both subsystems have a cascaded (or triangular) structure and it has turned out beneficial to choose the $\boldsymbol{e}_i$ to reflect this structure, i.e., the first components of the $\boldsymbol{e}_i$ are independent of θ_B or θ_S, respectively.

For obtaining the discrete time system (4) we use a sampling time of 2 seconds. For the discretization of each of the state spaces $\mathcal{X}_1$ and $\mathcal{X}_2$ from (30) we use a partition $\mathcal{P}$ of 8×8 equally sized rectangular elements. The target set $\mathcal{A}^V$ consists of the partition element containing the operating point (34), i.e., $\mathcal{A}_1^V = [0.33;\ 0.3475] \times [290.3375;\ 295.025]$ and $\mathcal{A}_2^V = [0.33;\ 0.3475] \times [296.9;\ 300.65]$, i.e., we choose a smaller set than $\mathcal{A}$ in (33). The stage costs are chosen as

$$g_1(\boldsymbol{x}_1, \boldsymbol{u}_1) = \frac{1}{0.0196}(l_B - 0.33)^2 + \frac{1}{1406.25}(\theta_B - 294.7)^2 \tag{39}$$

and

$$g_2(\boldsymbol{x}_2, \boldsymbol{u}_2) = \frac{1}{0.0196}(l_S - 0.34)^2 + \frac{1}{1406.25}(\theta_S - 300.2)^2. \tag{40}$$

For constructing the hypergraph we also need to discretize the control and perturbation input sets. We accomplish this by choosing the disturbances $\tilde{\boldsymbol{v}}_i \in \{-1;\, 0;\, 1\}^2$ and discretizing the control inputs for Σ_1 by 9×5 equidistant values and for Σ_2 by 9×4 equidistant values.

As mentioned in Section 3.4, an event is triggered whenever the state leaves a partition element. In order to algorithmically check whether this happens, we need to define a maximum number R of steps after which an element P is considered as not left, cf. the discussion after Definition 2.1 in Grüne & Müller (2009). Here we choose $R = 600$. In order to increase the efficiency of the algorithm we moreover use one step of past information for the controller design, for details see (Grüne & Müller, 2009, Section III) or (Grüne et al., 2010, Section 3.4).

The resulting approximated optimal value functions V_1 of Σ_1 (left) and V_2 of Σ_2 (right) depending on the initial value are depicted in Figure 7. One notes that the values of V_2 are much higher than those of V_1 because the cooling unit in reactor B is much slower than the heating unit in reactor S. This effect is also visible when looking at the maximal time needed to reach the target set from a given partition element which is shown in Figure 8.

6.6. Decentralized event-based controller resulting from the local approach

The local approach uses a linearized model of the continuous flow process. Therefore, the nonlinear system (28), (29) is linearized around the operating point (34) with

$$\bar{\boldsymbol{u}}_1 = \begin{pmatrix} \bar{u}_{\mathrm{T1}} \\ \bar{u}_{\mathrm{CU}} \end{pmatrix} = \begin{pmatrix} 0.5 \\ 0.5 \end{pmatrix}, \quad \bar{\boldsymbol{u}}_2 = \begin{pmatrix} \bar{u}_{\mathrm{T3}} \\ \bar{u}_{\mathrm{H}} \end{pmatrix} = \begin{pmatrix} 0.5 \\ 0.5 \end{pmatrix}.$$

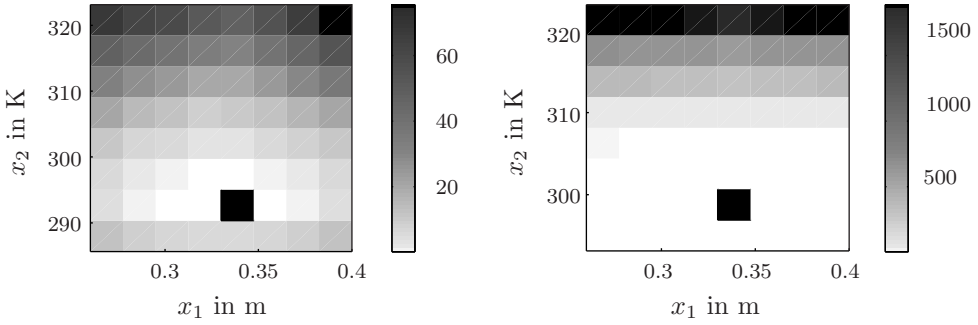

Figure 7: Value functions for Σ_1 (left) and Σ_2 (right) over state-space

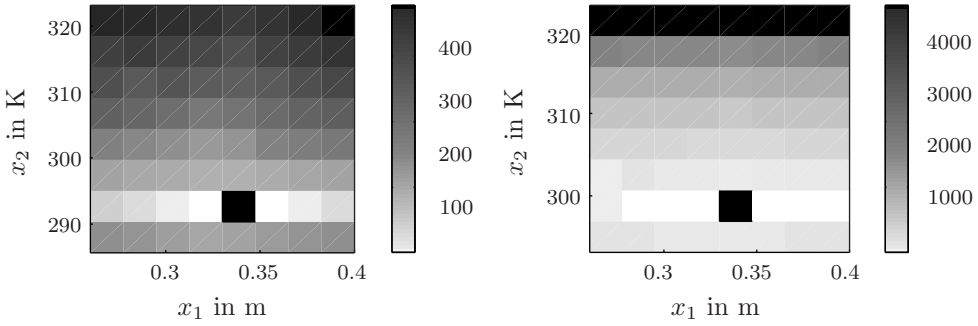

Figure 8: Maximal time in seconds to reach the target set for Σ_1 (left) and Σ_2 (right) over state-space

and the valve angles (35), (36). These settings yield the linearized model of the form (14), (15) for $i = 1, 2$ with

$$\boldsymbol{A}_1 = 10^{-3} \begin{pmatrix} -5.74 & 0 \\ -34.5 & -8.58 \end{pmatrix}, \quad \boldsymbol{A}_2 = 10^{-3} \begin{pmatrix} -5.00 & 0 \\ 39.2 & -5.58 \end{pmatrix}$$

$$\boldsymbol{B}_1 = 10^{-3} \begin{pmatrix} 2.30 & 0 \\ 0 & -38.9 \end{pmatrix}, \quad \boldsymbol{B}_2 = 10^{-3} \begin{pmatrix} 2.59 & 0 \\ 0 & 35.0 \end{pmatrix}$$

$$\boldsymbol{E}_1 = 10^{-3} \begin{pmatrix} 0 \\ 169 \end{pmatrix}, \quad \boldsymbol{E}_2 = 10^{-3} \begin{pmatrix} 1.16 \\ -20.7 \end{pmatrix}$$

$$\boldsymbol{E}_{\mathrm{s}1} = 10^{-3} \begin{pmatrix} 2.42 & 0 \\ 43.9 & 5.44 \end{pmatrix}, \quad \boldsymbol{E}_{\mathrm{s}2} = 10^{-3} \begin{pmatrix} 2.85 & 0 \\ -46.5 & 5.58 \end{pmatrix}$$

$$\boldsymbol{C}_{\mathrm{z}1} = \begin{pmatrix} 1 & 0 \\ 0 & 1 \end{pmatrix}, \qquad \boldsymbol{C}_{\mathrm{z}2} = \begin{pmatrix} 1 & 0 \\ 0 & 1 \end{pmatrix}$$

and the interconnections

$$\boldsymbol{L}_{12} = \begin{pmatrix} 1 & 0 \\ 0 & 1 \end{pmatrix}, \quad \boldsymbol{L}_{21} = \begin{pmatrix} 1 & 0 \\ 0 & 1 \end{pmatrix}.$$

The control input generators C_1 and C_2 determine the control inputs according to the model (17) using the feedback gains

$$\boldsymbol{K}_1 = \begin{pmatrix} 10.5 & 0 \\ 0.90 & -0.05 \end{pmatrix}, \quad \boldsymbol{K}_2 = \begin{pmatrix} 11.5 & 0 \\ 1.10 & 0.40 \end{pmatrix}. \tag{41}$$

With these parameters the stability test (20) yields

$$\lambda_{\mathrm{P}} \left(\int_0^\infty \bar{\boldsymbol{G}}_{\mathrm{xs}}(t) \bar{\boldsymbol{L}} \bar{\boldsymbol{C}}_{\mathrm{z}} \mathrm{d}t \right) = 0.38 < 1$$

which implies ultimate boundedness of the overall closed-loop system. Moreover, the stability condition (20) can be used to show that the event-based control system is robustly stable with respect to changes of the coupling strength. The evaluation of the condition (20) for the interconnection

$$\boldsymbol{L} = \kappa \begin{pmatrix} \boldsymbol{O} & \boldsymbol{L}_{12} \\ \boldsymbol{L}_{21} & \boldsymbol{O} \end{pmatrix}, \tag{42}$$

in dependence upon a scaling factor $\kappa \in \mathbb{R}_+$ yields that the overall system is UB for $0 \leq \kappa < \kappa_{\mathrm{crit}} = 2.6$.

In order to satisfy the control aim (3) with the target set $\mathcal{A} = \mathcal{A}_1 \times \mathcal{A}_2$ as defined in (33), the event threshold vectors of the event generators E_1 and E_2 are chosen to

$$\bar{\boldsymbol{e}}_1 = \begin{pmatrix} 0.02 \\ 0.4 \end{pmatrix}, \quad \bar{\boldsymbol{e}}_2 = \begin{pmatrix} 0.02 \\ 0.4 \end{pmatrix}, \tag{43}$$

which means that E_1 and E_2 trigger an event if either the level or the temperature deviates by 2 cm or 0.4 K, respectively, from the corresponding model state. According to Eqs. (25)–(27), the choice (43) yields the ultimate bound

$$\boldsymbol{b} = (0.018 \;\; 2.56 \;\; 0.027 \;\; 1.36)^\top .$$

Hence, the local approach ensures that the state $\boldsymbol{x} = (l_\mathrm{B} \; \vartheta_\mathrm{B} \; l_\mathrm{S} \; \vartheta_\mathrm{S})^\top$ is kept within the bounds

$$l_\mathrm{B}(t) \in [0.312; 0.348], \quad \vartheta_\mathrm{B}(t) \in [292.1; 297.3] \tag{44a}$$

$$l_\mathrm{S}(t) \in [0.313; 0.367], \quad \vartheta_\mathrm{S}(t) \in [298.8; 301.6] \tag{44b}$$

for all $t \geq T(\boldsymbol{x}_0)$ where the time $T(\boldsymbol{x}_0)$ is determined by the global approach. A comparison of the bounds (44) with the desired target set (33) shows that the decentralized event-based controllers with state-feedback gains (41) and the event thresholds (43) satisfy the control aim.

The event generators E_1 and E_2 are implemented as in (19) with the event condition

$$\left\| |\boldsymbol{x}_{\Delta i}(t)| - \bar{\boldsymbol{e}}_i \right\|_\infty \geq 0 \tag{45}$$

for $i = 1, 2$. For the practical realization, the inequality (45) substitutes the equality (18) as due to the implementation on digital hardware the event

condition is checked periodically with sampling period $T_\mathrm{s} = 0.3\,\mathrm{s}$ which generally only detects the exceeding of the condition. Nevertheless, in relation to the time constants of the process the sampling is fast and, thus, the error that is introduced by the sampling is negligible. A more detailed analysis of event-based control with discrete-time sampling is given in Grüne et al. (2010).

6.7. Implementation of the event-based controllers

Each of the previously explained components of the decentralized event-based controllers is implemented in MATLAB/Simulink using the concept of Level-2 MATLAB S-Functions. The implementations of the control input generator and event generator is independent of the index of the subsystem to which these components are assigned and, therefore, the index is omitted for the following explanations.

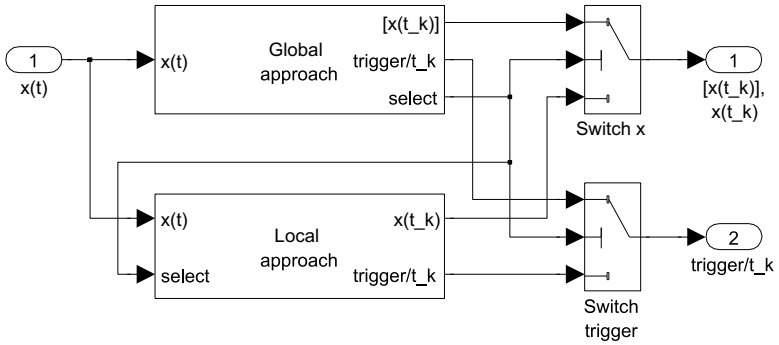

Figure 9: Simulink model of the event generator

Figure 9 illustrates the structure of the Simulink model representing an event generator, including the blocks `Global approach` and `Local approach`. The blocks `Switch x` and `Switch trigger` are used to route the signals of

`Global approach` and `Local approach` where the criteria for passing the first input is `select` ≥ 1 in both switches. The block `Global approach` determines the integer value $[\boldsymbol{x}(t_k)]$ that uniquely identifies the box in which the current state is. The signal `trigger/t_k` is updated to the current event time t_k whenever the state $\boldsymbol{x}(t)$ passes from one box to another (i. e. whenever an event is generated). The block `Global approach` detects the time instant $t = T$ at which the state $\boldsymbol{x}(t)$ enters the target set $\mathcal{A}$. At this time the block `Global approach` switches `select` from `1` to `0`, indicating the activation of the block `Local approach` which then sets `trigger/t_k = -T`. The transmission of the current state $\boldsymbol{x}(T)$ and the time $t_k = -T$ to the control input generator signalizes the switching to the local approach by virtue of the negative event time. From then on, the block `Local approach` generates events according to the condition (45) and whenever this condition is satisfied it sets `trigger/t_k =` t_k.

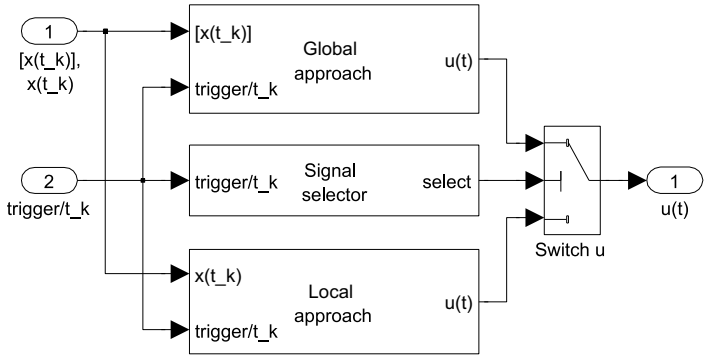

Figure 10: Simulink model of the control input generator

The structure of the Simulink model of the control input generator is depicted in Fig. 10. Similar to the model of the event generator, the main components are the blocks `Global approach` and `Local approach`. The

first one determines the control input $\boldsymbol{u}(t)$ by selecting at the event times the appropriate entry from a look-up table which is linked to the integer $[\boldsymbol{x}(t_k)]$. In the block `Local approach` the information $\boldsymbol{x}(t_k)$ received at the event time t_k is used to reinitialize the state of a model that is applied for the input generation. The decision whether the control input generated by the `Global approach` or by the `Local approach` shall be applied is implemented in the Embedded MATLAB Function `Signal selector`. third input of the block `Switch u`.

7. Experimental evaluation

7.1. Description of the experiment

This section presents the results of an experiment where the state $\boldsymbol{x}(t)$ of the system (28), (29) is driven from the initial state

$$\boldsymbol{x}_1(0) = \begin{pmatrix} l_{\mathrm{B}}(0) \\ \vartheta_{\mathrm{B}}(0) \end{pmatrix} = \begin{pmatrix} 0.40 \\ 317.2 \end{pmatrix}, \quad \boldsymbol{x}_2(0) = \begin{pmatrix} l_{\mathrm{S}}(0) \\ \vartheta_{\mathrm{S}}(0) \end{pmatrix} = \begin{pmatrix} 0.40 \\ 293.4 \end{pmatrix}$$

to the target set $\mathcal{A}$ as defined in (33) and maintained there. For the transition of the state $\boldsymbol{x}(t)$ to the set $\mathcal{A}$ the system is considered to be undisturbed, whereas the disturbances $\boldsymbol{d}(t)$ are temporarily active while the state $\boldsymbol{x}(t)$ is to be kept within $\mathcal{A}$. The disturbance characteristics are set to

$$\begin{aligned} d_{\mathrm{H}}(t) &= 0.1, \qquad \text{for } 800 \leq t \leq 1200, \\ d_{\mathrm{F}}(t) &= 0.25, \quad \text{for } 1550 \leq t \leq 1800. \end{aligned}$$

In the remaining time intervals no disturbance is active.

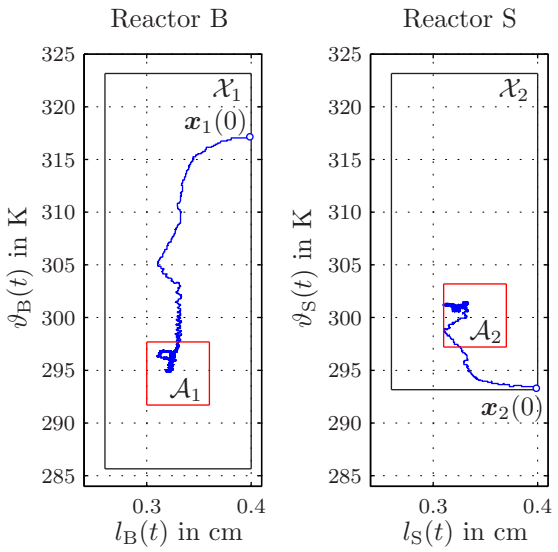

Figure 11: Trajectories of the state $\boldsymbol{x}_1(t)$ and $\boldsymbol{x}_2(t)$

7.2. Experimental results

The behavior of the continuous flow process with decentralized event-based control is illustrated in Figs. 11–14. Figure 11 gives an overview over the transition of the subsystem states $\boldsymbol{x}_1(t)$ and $\boldsymbol{x}_2(t)$ into the respective target regions. Once, the states enter the target regions, they are kept within these sets which shows that the control aim is fulfilled. Note that this aim is achieved despite model uncertainties which occur, since the model (28), (29) does not precisely describe the behavior of the plant. Hence, this investigation shows that both proposed decentralized event-based control approaches are robust with respect to model uncertainties.

The transition of the state into the target region $\mathcal{A}$ by the global approach is shown in Fig. 12. In reactor B the target region $\mathcal{A}_1$ is reached within $T_1 = 398\,\mathrm{s}$, while in reactor S the state $\boldsymbol{x}_2(t)$ enters $\mathcal{A}_2$ already after $T_2 = 103\,\mathrm{s}$. The state $\boldsymbol{x}_2(t)$ is steered by four times faster to the target region $\mathcal{A}_2$

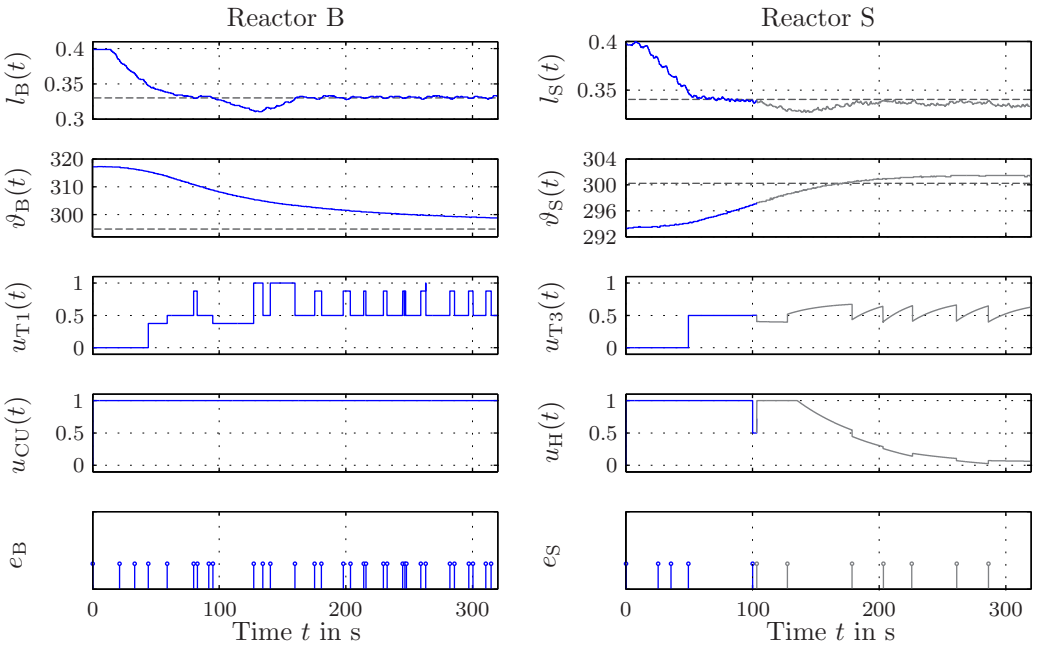

Figure 12: Behavior of the global approach. In the upper two rows the trajectories of the levels $l_B(t), l_S(t)$ and of the temperatures $\vartheta_B(t), \vartheta_S(t)$ are shown for reactor B and S on the left-hand side or right-hand side, respectively. The next two rows depict the respective control inputs and the event time instant are marked by stems in the bottom figures.

compared to the transition of $\boldsymbol{x}_1(t)$ to $\mathcal{A}_1$, which is due to the fact that $\boldsymbol{x}_2(0)$ is much closer to $\mathcal{A}_2$ as $\boldsymbol{x}_1(0)$ is to $\mathcal{A}_1$. This is also reflected in the number of events triggered in both subsystems: In the reactor S only 5 events are triggered before the local approach is activated, whereas in reactor B, 48 events are generated before the target set $\mathcal{A}_1$ is reached.

Figure 13 shows the disturbance rejection behavior of the continuous flow process with the local event-based control approach. The time intervals in which the disturbances $d_H(t)$ and $d_F(t)$ are active are highlighted in gray. The experiments show that in event-based control the feedback communication

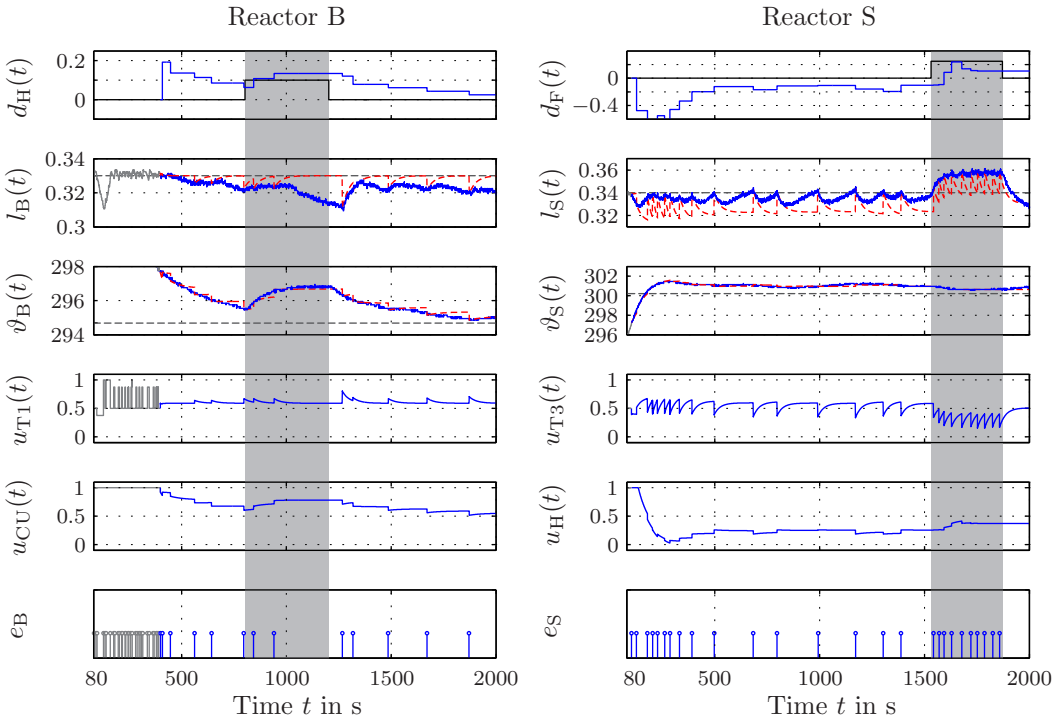

Figure 13: Disturbance rejection behavior of the local approach. The behavior of reactor B and reactor S is depicted in the plots on the left-hand side or right-hand side, respectively. The first row shows the disturbances and the estimated values. The trajectories of the level and temperature are given in the second and third row (solid line: plant state, dashed line: model state). The control inputs are illustrated in the next two rows and the event time instants are represented by stems in the bottom figure.

is adapted to the current system behavior. In the time interval $[103\,\mathrm{s}, 398\,\mathrm{s}]$, the state $\boldsymbol{x}_2(t)$ is in the target set $\mathcal{A}_2$, whereas $\boldsymbol{x}_1(t)$ is still outside of $\mathcal{A}_1$, which means that reactor S is considerably affected by reactor B via the interconnections. In this time interval, 9 events are generated in reactor S within less than 300 s, while in $[398\,\mathrm{s}, 1550\,\mathrm{s}]$, where the coupling effect is small and the disturbance d_{F} is not active, only 7 events are triggered in more

than 1150 s. In order to attenuate the disturbance $d_{\mathrm{F}}(t)$ that affects reactor S in the gray highlighted interval, the feedback communication is induced more often, i. e. 10 events are generated. In total, only 13 events per 1602 s are triggered in reactor B and 26 events per 1897 s are triggered in reactor S. Compared to a sampled-data control with a sampling period $T_{\mathrm{s}} = 10\,\mathrm{s}$ (which is a typical choice for the considered continuous flow process), the feedback communication effort is considerably reduced by the event-based control.

Figure 14 provides a verification of the bounds (44) determined according to the analysis method in Theorem 4. It is shown that in both subsystems, the levels $l_{\mathrm{B}}(t)$ and $l_{\mathrm{S}}(t)$ exceed the calculated bounds, nevertheless, the maximum deviation between the levels and the respective bounds is less than 0.03 cm. From this investigation it can be concluded that the analysis method in Theorem 4 yields tight bounds for the considered class of systems, however, these bounds might not hold in the presence of model uncertainties.

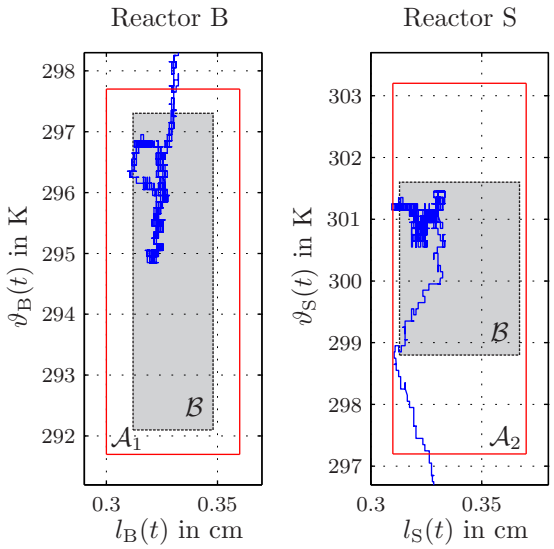

Figure 14: Verification of the ultimate boundedness analysis

8. Conclusion

This paper has presented a new method for the decentralized event-based control of physically interconnected systems and its practical application to a continuous flow process. The proposed control method is based on two approaches, referred to as global and local approach, that differ with respect to their control task for which they are specially designed. The global approach uses a nonlinear model of the plant and quantized state information in order to drive the state of each system into a target region. The state is kept within this target set in spite of exogenous disturbances and interconnections to other systems by the local approach, where a feedback is only invoked if the state deviates from a state estimate, determined using a linearized plant model, by some threshold. In this way, both approaches jointly achieve ultimate boundedness of the closed-loop system. The theoretical results have been evaluated on the basis of experimental results, obtained by the application of the control method to a continuous flow process. These results have mainly shown two facts: First, the decentralized event-based control method is robust with respect to model uncertainties and, second, the control aim is accomplished with considerably less feedback communication effort compared to the communication in sampled-data control.

Acknowledgements

This work is supported by the German Research Foundation (DFG) within the priority program "Control Theory of Digitally Networked Dynamical Systems", grant numbers LU 462/26-2 and GR 1569/11-2 and by

the European Union under the 7th Framework Programme FP7–PEOPLE–2010–ITN, Grant agreement nr. 264735–SADCO.

References

Arzén, K. (1999). A simple event-based PID controller. In *Proc. 14th IFAC World Congress* (pp. 423–428).

Åström, K. J., & Bernhardsson, B. (1999). Comparison of periodic and event-based sampling for first-order stochastic systems. In *Proc. 14th IFAC World Congress* (pp. 301–306).

Dashkovskiy, S. N., Rüffer, B. S., & Wirth, F. R. (2010). Small gain theorems for large scale systems and construction of ISS Lyapunov functions. *SIAM J. Control Optim.*, *48*, 4089–4118.

De Persis, C., Sailer, R., & Wirth, F. (2011). On a small-gain approach to distributed event-triggered control. In *Proc. 14th IFAC World Congress* (pp. 2401–2406).

Donkers, M. C. F., & Heemels, W. P. M. H. (2012). Output-based event-triggered control with guaranteed $\mathcal{L}_\infty$-gain and improved decentralised event-triggering. *IEEE Transactions on Automatic Control*, *57*, 1362–1376.

Garcia, E., & Antsaklis, P. J. (2011). Model-based event-triggered control with time-varying network delays. In *Proc. Joint IEEE Conference on Decision and Control and European Control Conference* (pp. 1650–1655).

Garcia, E., & Antsaklis, P. J. (2012). Decentralized model-based event-triggered control of networked systems. In *Proc. American Control Conference* (pp. 6485–6490).

Gawthrop, P. J., & Wang, L. B. (2009). Event-driven intermittent control. *International Journal of Control*, *82*, 2235–2248.

Grüne, L., Jerg, S., Junge, O., Lehmann, D., Lunze, J., Müller, F., & Post, M. (2010). Two complementary approaches to event-based control. *Automatisierungstechnik*, *58*, 173–182.

Grüne, L., & Junge, O. (2007). Approximately optimal nonlinear stabilization with preservation of the Lyapunov function property. In *Proc. IEEE Conference on Decision and Control* (pp. 702–707).

Grüne, L., & Junge, O. (2008). Global optimal control of perturbed systems. *J. Optim. Theory Appl.*, *236*, 411–429.

Grüne, L., & Müller, F. (2009). An algorithm for event-based optimal feedback control. In *Proc. IEEE Conference on Decision and Control* (pp. 5311 – 5316).

Grüne, L., & Sigurani, M. (2013). Numerical ISS controller design via a dynamic game approach. In *Proc. IEEE Conference on Decision and Control*. To appear.

Heemels, W. P. M. H., Gorter, R. J. A., van den Bosch, P. P. J., Weiland, S., Hendrix, W. H. A., & Vonder, M. R. (1999). Asynchronous measurement and control: A case study on motor synchronization. *Control Engineering Practice*, *7*, 1467–1482.

Hendricks, E., Jensen, M., Chevalier, A., & Vesterholm, T. (1994). Problems in event based engine control. In *Proc. American Control Conference* (pp. 1585–1587).

Henningsson, T., & Cervin, A. (2009). Comparison of lti and event-based control for a moving cart with quantized position measurement. In *Proc. European Control Conference* (pp. 3791–3796).

Henningsson, T., Johannesson, E., & Cervin, A. (2008). Sporadic event-based control of first-order linear stochastic systems. *Automatica*, *44*, 2890–2895.

Jiang, Z.-P., & Wang, Y. (2001). Input-to-state stability for discrete-time nonlinear systems. *Automatica*, *37*, 857–869.

Junge, O., & Osinga, H. M. (2004). A set oriented approach to global optimal control. *ESAIM Control Optim. Calc. Var.*, *10*, 259–270 (electronic).

Khalil, H. K. (2002). *Nonlinear Systems*. Prentice Hall, Upper Saddle River.

Kwon, W. H., Kim, Y. H., Lee, S. J., & Paek, K. (1999). Event-based modelling and control for the burnthrough point in sintering processes. *IEEE Transactions on Control Systems Technology*, *7*, 31–41.

Lehmann, D. (2011). *Event-Based State-Feedback Control*. Logos-Verlag, Berlin.

Lehmann, D., & Lunze, J. (2011). Extension and experimental evaluation of an event-based state-feedback approach. *Control Engineering Practice*, *19*, 101–112.

Lunze, J. (1992). *Feedback Control of Large-Scale Systems*. Prentice Hall, London.

Lunze, J., & Lehmann, D. (2010). A state-feedback approach to event-based control. *Automatica*, *46*, 211–215.

Mazo, M., & Tabuada, P. (2010). Decentralized event-triggered control over wireless sensor/actuator networks. *IEEE Transactions on Automatic Control*, *56*, 2456–2461.

Molin, A., & Hirche, S. (2013). On the optimality of certainty equivalence for event-triggered control systems. *IEEE Transactions on Automatic Control*, *58*, 470–474.

Sandee, J. H., Heemels, W. P. M. H., Hulsenboom, S. B. F., & van den Bosch, P. P. J. (2007). Analysis and experimental validation of a sensor-based event-driven controller. In *Proc. American Control Conference* (pp. 2867–2874).

Stöcker, C., & Lunze, J. (2011). Event-based control of nonlinear systems: An input-output linearization approach. In *Proc. Joint IEEE Conference on Decision and Control and European Control Conference* (pp. 2541–2546).

Stöcker, C., & Lunze, J. (2013). Input-to-state stability of event-based state-feedback control. In *Proc. European Control Conference* (pp. 1145–1150).

Stöcker, C., Vey, D., & Lunze, J. (2013). Decentralized event-based control: Stability analysis and experimental evaluation. *Nonlinear Analysis: Hybrid Systems*, . To be published.

Tabuada, P. (2007). Event-triggered real-time scheduling of stabilizing control tasks. *IEEE Transactions on Automatic Control*, *52*, 1680–1685.

Tallapragada, P., & Chopra, N. (2011). On event triggered trajectory tracking for control affine nonlinear systems. In *Proc. Joint IEEE Conference on Decision and Control and European Control Conference* (pp. 5377–5382).

Trimpe, S., & D'Andrea, R. (2011). An experimental demonstration of a distributed and event-based state estimation algorithm. In *Proc. 18th IFAC World Congress* (pp. 8811–8818).

Wang, X., & Lemmon, M. D. (2011a). Attentively efficient controllers for event-triggered feedback systems. In *Proc. Joint IEEE Conference on Decision and Control and European Control Conference* (pp. 4698–4703).

Wang, X., & Lemmon, M. D. (2011b). Event-triggering in distributed networked control systems. *IEEE Transactions on Automatic Control*, *56*, 586–601.

Wang, X., & Lemmon, M. D. (2012). On event design in event-triggered feedback systems. *Automatica*, *47*, 2319–2322.

Yook, J. K., Tilbury, D. M., & Soparkar, N. R. (2002). Trading computation for bandwidth: reducing communication in distributed control systems using state estimators. *IEEE Transactions on Control Systems Technology*, *10*, 503–518.

Yu, H., & Antsaklis, P. J. (2011). Event-triggered real-time scheduling for stabilization of passive and output feedback passive systems. In *Proc. American Control Conference* (pp. 1674–1679).